Glyphosate Inhibits Melanization and Increases Insect Susceptibility to Infection

Daniel F. Q. Smith[1], Emma Camacho[1], Raviraj Thakur[2], Alexander J. Barron[3], Nichole A. Broderick[3], Arturo Casadevall[1,4*]

[1]Department of Molecular Microbiology and Immunology, Johns Hopkins Bloomberg School of Public Health, [2] Department of Otolaryngology, Head and Neck Surgery, Johns Hopkins Medicine, Baltimore, MD 21205, [3] Department of Molecular and Cell Biology, University of Connecticut, Storrs, CT 06269, United States of America. [4] Lead Contact

Running title: Glyphosate Inhibits Melanization in Insects and Fungi

SUMMARY

Melanin is a black-brown pigment found throughout all kingdoms of life playing diverse roles including: UV protection, thermoregulation, oxidant scavenging, arthropod immunity, and microbial virulence. Given melanin's broad functions in the biosphere, particularly in insect immune defenses, it is important to understand how environmental conditions affect melanization. Glyphosate, the most widely used herbicide, inhibits melanin production. Here we elucidate the mechanism underlying glyphosate's inhibition of melanization demonstrate the herbicide's multifactorial effects on insects. Glyphosate acts as an antioxidant and disrupts the oxidation-reduction balance of melanization. The drug reduced wax moth larvae survival after infection, increased parasite burden in malaria-transmitting mosquitoes, and altered midgut microbiome composition in adult mosquitoes. These findings suggest that glyphosate's environmental accumulation could contribute to the so called insect apocalypse, characterized by species declines, by rendering them more susceptible to microbial pathogens due to melanization inhibition, immune impairment, and perturbations in microbiota composition.

Key Words: melanin, fungi, tyrosinase, phenol oxidase, malaria, midgut microbiome, *Galleria*, *Anopheles*

INTRODUCTION

* Correspondance: acasade1@jhu.edu

Melanin is produced through a series of oxidation and reduction reactions, which are typically catalyzed by two distinct classes of enzymes: laccases (EC. 1.10.3.2) and phenol oxidases, the latter is divided into tyrosinases (EC. 1.14.18.1) and catechol oxidases (EC. 1.10.3.1) (Whitten and Coates, 2017). Tyrosinases are copper metalloenzymes found throughout nature in fungi, protists, arthropods, birds, and mammals, and are responsible for two catalytic roles: 1) hydroxylation of monophenols into *ortho*-diphenols, followed by 2) two-electron oxidation of *ortho*-catechols into *ortho*-quinones (Ramsden and Riley, 2014). In melanin biosynthesis, tyrosinase first converts 3,4-dihydroxyphenylalanine (L-DOPA) into dopaquinone (DQ), which then undergoes a series of spontaneous oxidation and reduction reactions resulting in dopachrome, then dihydroxyindole (DHI) DHI undergoes a free-radical mediated polymerization that yields black-brown pigments known as eumelanins (Christensen et al., 2005; Ramsden and Riley, 2014).

In arthropods, including insects, melanogenesis is one of the key components of the immune response (Christensen et al., 2005). Upon invasion by a foreign organism, the insect's complement-like system launches a protease cascade, which cleaves pro-phenol oxidases into the active phenol oxidases (POs). POs convert dopamine, *N*-acetyldopamine, and catecholamines in hemolymph into melanin on the surface of the pathogen (Christensen et al., 2005; González-Santoyo and Córdoba-Aguilar, 2012; Marmaras et al., 1996). This process eliminates the pathogen through exposure to reactive oxygen species (ROS), nutrient deprivation, and lysis from toxic melanin intermediates (Zhao et al., 2011; Nappi and Christensen, 2005; Chen and Chen, 1995). In insects, the melanin-based immune response represents a major effector mechanism, thus it is important to understand how common environmental compounds could inhibit or enhance melanin production.

Glyphosate (GLYPH) is a widespread herbicide found in the environment, and interferes with melanization in the fungus *Cryptococcus neoformans* (Nosanchuk et al., 2001). *C. neoformans* produces melanin, which functions as a virulence factor to resist host defenses and environmental threats (Almeida et al., 2015; Smith and Casadevall, 2019; Wang et al., 1995) . Treatment with GLYPH prevented fungal melanization *in vitro* and reduced fungal virulence in murine infection models (Nosanchuk et al., 2001). Other aminophosphonic acids inhibit fungal eumelanin in the human pathogen *Aspergilius flavus* (Dzhavakhiya et al., 2016). Further, this class of compounds are patented for use in human cosmetics, and are marketed as solutions to inhibit melanogenesis in the skin (Yu and Scott, 2008; Seguin and Babizhayev, 2001).

GLYPH, a phosphonic analogue of glycine, is the active ingredient in Roundup herbicide (Samsel and Seneff, 2016). It kills plants through competitive inhibition of 5-

enolpyruvylshikimate-3-phosphate (EPSP) synthase in the shikimate pathway, which is responsible for aromatic amino acid synthesis is many plants, fungi, and bacteria (Duke and Powles, 2008). The development of GLYPH-resistant genetically modified crops, named Roundup Ready crops (Dill, 2008), enable farmers to spray large amounts of GLYPH on their fields to selectively kill unwanted plants (Gianessi, 1999). Since their introduction (1996), global use of GLYPH directly related to GMO agriculture has increased substantially, up to 12-fold between 1996 and 2014, including 8-fold in the US, 134-fold in Brazil, and 107-fold in Argentina (Benbrook, 2012, 2016)[·]. While the use of GLYPH continues to spread, some nations have severely restricted its use due to reports and court rulings linking GLYPH to human disease and toxicity (Guyton et al., 2015; Barbosa et al., 2001; Jayasumana et al., 2014). These findings are controversial (Robinson, 2012) and refuted by the original manufacturer, citing large studies showing no correlation between glyphosate and cancer (Andreotti et al., 2018). Beyond direct impacts on human health there is great interest to understand environmental impacts.

Following application, herbicide washes into soil and water supplies. In agriculture settings, GLYPH is commonly applied at concentrations of ~28 to 57 mM (Bott et al., 2008) with a half-life that varies from days to months (Saunders and Pezeshki, 2015; Mercurio et al., 2014; Edwards et al., 1980). More than 88% of the GLYPH applied to fields remains in the top 10 cm of soil (Lupi et al., 2019), where it can disrupt microbial populations and crop health by increasing plant susceptibility to phytopathogens (Yamada et al., 2009), and alter plant nutrient acquisition by perturbing fungi-plant rhizosphere symbioses (Johal and Huber, 2009). GLYPH is a reported contaminant in water bodies at concentrations that range from 1 nM to 30 μM (Edwards et al., 1980; Brauman et al., 2011), and can have a negative impact on the survival and success of algae and aquatic organisms (Tsui and Chu, 2003). More recently, GLYPH was shown to enhance the susceptibility of honeybees to infection with *Serratia marcescens*, attributed to microbiome alterations (Motta et al., 2018). Similarly, GLYPH disrupts folate production in the tsetse fly's obligate midgut bacterium *Wigglesworthia,* an important factor needed for *Trypanosoma brucei* to infect the insect (Rio et al., 2019).

In this paper, we examine GLYPH's mechanism of melanin inhibition using an *in vitro* mushroom tyrosinase model, and validate GLYPH as an inhibitor of insect melanogenesis using *Galleria mellonella* and *Anopheles gambiae*. We further characterize the effects of GLYPH on *G. mellonella* susceptibility to *C. neoformans* infection, and *A. gambiae* susceptibility to *Plasmodium falciparum* infection. Our results indicate that GLYPH can be a major immune modulator of insects through its effect on melanization.

RESULTS

GLYPH Inhibits Dopaquinone Production

To investigate how glyphosate (GLYPH) inhibited melanization, we evaluated the formation of melanin intermediates in a step-wise manner using a commercially available fungal tyrosinase. Although this tyrosinase differs from insect PO, the melanization reaction in these systems follows the same Mason-Raper pathway (Mason, 1948; Raper, 1927). First, L-DOPA is oxidized into dopaquinone (DQ) enzymatically or spontaneously (García-Borrón and Sánchez, 2011). Using L-DOPA with and without tyrosinase, we monitored the initial step of melanin production in a controlled system, and tested the effects of GLYPH on the reaction. Quinones like DQ are unstable and difficult to study directly; thus, DQ quantification relies on the formation of a stable adduct with MBTH (3-methyl-2-benxothiaxolinone hydrazine) that forms a pigment that absorbs at 505 nm (Winder and Harris, 1991). This absorption overlaps with the absorption of another melanin intermediate, dopachrome (DC), but is not expected to interfere since DQ reaction with MBTH prevents DC formation. Further, the molar absorbance coefficient for MBTH-DQ is more than 10 times higher (39,000 L/[mol cm]) than that of DC (3,700 L/[mol cm]), and interference from DC would be relatively small.

We found that GLYPH inhibits DQ production in a dose-dependent manner (Fig. 1a). This inhibition is seen in the tyrosinase-mediated oxidation and auto-oxidation of L-DOPA. It appears that the inhibition in the tyrosinase reaction is due to inhibited background auto-oxidation, which when taken into account suggests no inhibition of DQ attributable to tyrosinase inhibition or altered enzyme function.

GLYPH Inhibits Production of Dopachrome and Melanin

DQ spontaneously cyclizes to form cyclodopa, which then undergoes a redox exchange with another DQ molecule to form one molecule of DC and one reformed molecule of L-DOPA. DC is a pink-orange pigment with absorbance maximum at 475 nm and is a useful proxy product for tyrosinase-mediated reaction kinetics (Jara et al., 1988). The rate of DC formation and the amount of DC produced were determined by measuring changes in absorbance during a reaction between L-DOPA and tyrosinase. There was a strong dose-dependent inhibition of DC level and rates of formation with GLYPH (Fig. 1b), implying that the compound's inhibitory effects were upstream of DC.

We tracked the reaction over 5 d to confirm inhibition of melanin itself. GLYPH inhibited the production of a black pigment dose-dependently, as measured by the absorbance of the tyrosinase reaction on Day 5 (Fig. 1c). Interestingly, GLYPH also inhibited the formation of

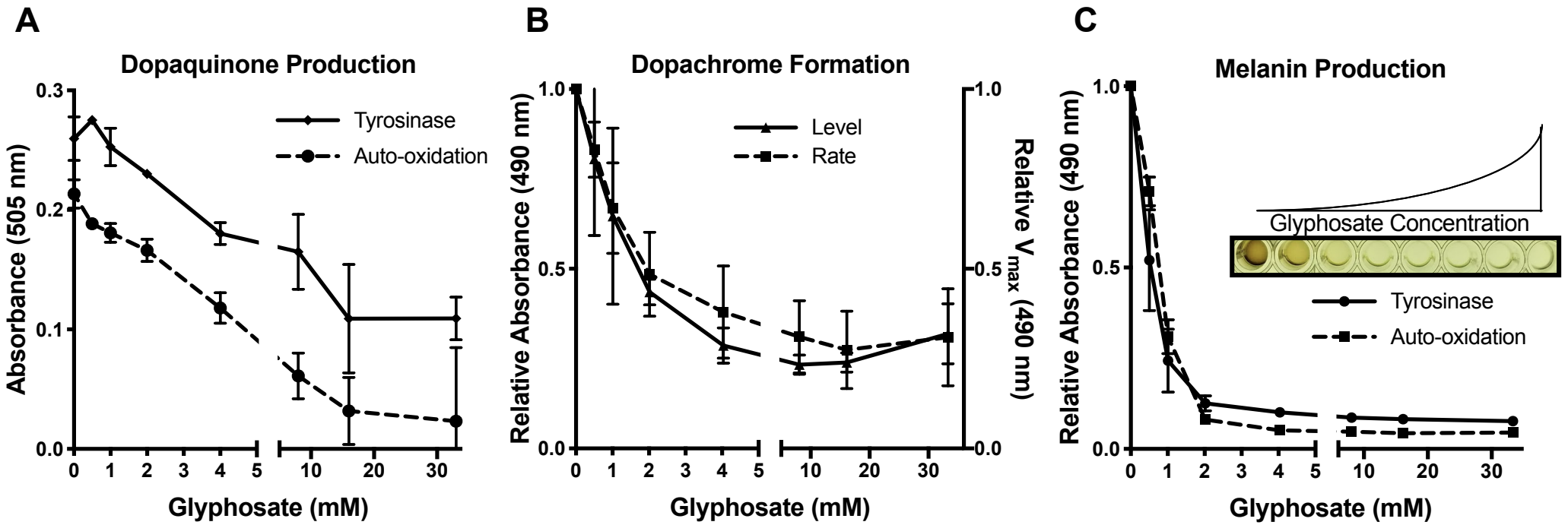

Fig. 1. ***GLYPH inhibits in vitro Melanin Production.*** **(A)** GLYPH inhibits formation of DQ produced by tyrosinase-mediated and spontaneous oxidation of L-DOPA. DQ is indicated by the absorbance of an MBTH-DQ adduct pigment at 505 nm. Absorption levels are shown relative to the no GLYPH control with background (MBTH mixture) subtracted after 1 h at 30ºC **(B)** GLYPH decreases the rate of DC formation and inhibits DC production from tyrosinase oxidation of L-DOPA. Rate of DC formation is the reaction V_{max} at 490 nm relative to the V_{max} without GLYPH. DC production is shown as the absorbance at 490 nm relative to the control after 30 min of reaction. **(C)** Melanin production is inhibited by GLYPH with tyrosinase and auto-oxidation of L-DOPA. Melanin levels are measured as the absorbance at 490 nm after 5 d of reaction. Values are depicted relative to the no GLYPH control. Error bars represent ±SD. Each experiment was performed at least three independent replicates.

pigment that derives from auto-oxidation of L-DOPA (Fig. 1c). This implies that GLYPH inhibited pigment production non-enzymatically.

Phosphate-Containing Compounds Inhibited Melanization Similarly to GLYPH

To gain insight into the features of GLYPH that inhibited melanogenesis we assayed several structurally similar compounds. To test the effect of the amino acid functional group, we compared GLYPH alongside to its non-phosphate analog, glycine. We also tested the inhibitory effects of phosphoserine and serine on melanin production. Phosphoserine inhibited melanization to nearly the same extent as GLYPH (Fig. 2a-c). In contrast, neither glycine nor serine inhibited DQ formation (Fig. 2a), DC formation (Fig. 2b), or overall melanin formation (Fig. 2c). We tested the inhibitory effects of organophosphate (phosphonoacetic acid), phosphoester (pyrophosphate), and phosphoric acid. All of the phosphate containing compounds inhibited DQ production (Fig. 2a) and DC formation (Fig. 2b) in a manner nearly identical to GLYPH, but differed slightly from each other in melanin inhibition.

Similar to GLYPH, these compounds all inhibited auto-oxidation of L-DOPA comparably to their inhibition of enzyme-mediated melanin production (Fig. 2e). This further illustrates that GLYPH and similar compounds inhibit melanin in a non-enzymatic fashion.

GLYPH Did Not React Directly With L-DOPA

We considered the possibility that GLYPH inhibited melanogenesis and DQ production by reacting with the L-DOPA substrate. To measure the reaction between these compounds, we analyzed mixtures of L-DOPA and GLYPH by ^{1}H-NMR and ^{31}P-NMR. We found no evidence of interaction between the two compounds based on peak shifts of hydrogen and phosphorous at both high (60 mM GLYPH and 20 mM L-DOPA) and low concentrations (6 mM GLYPH and 5 mM L-DOPA) (Fig. S1).

GLYPH Does Not Inhibit Tyrosinase Directly

If GLYPH was inhibiting melanin production through the formation of a covalent bond with tyrosinase, then inhibition should be irreversible. To test this, we treated 20 µg/ml tyrosinase with 5.63 mg/ml (33.33 mM) GLYPH, and removed the GLYPH by dialysis. The GLYPH-treated enzyme had similar activity to the control (Fig. 3a), making a strong case against a mechanism whereby GLYPH inhibited melanogenesis through irreversible inhibition of tyrosinase. Instead, analysis of the tyrosinase reaction by Michaelis-Menten kinetics assay with L-DOPA and GLYPH suggested that GLYPH is a non-competitive inhibitor of melanin and DC

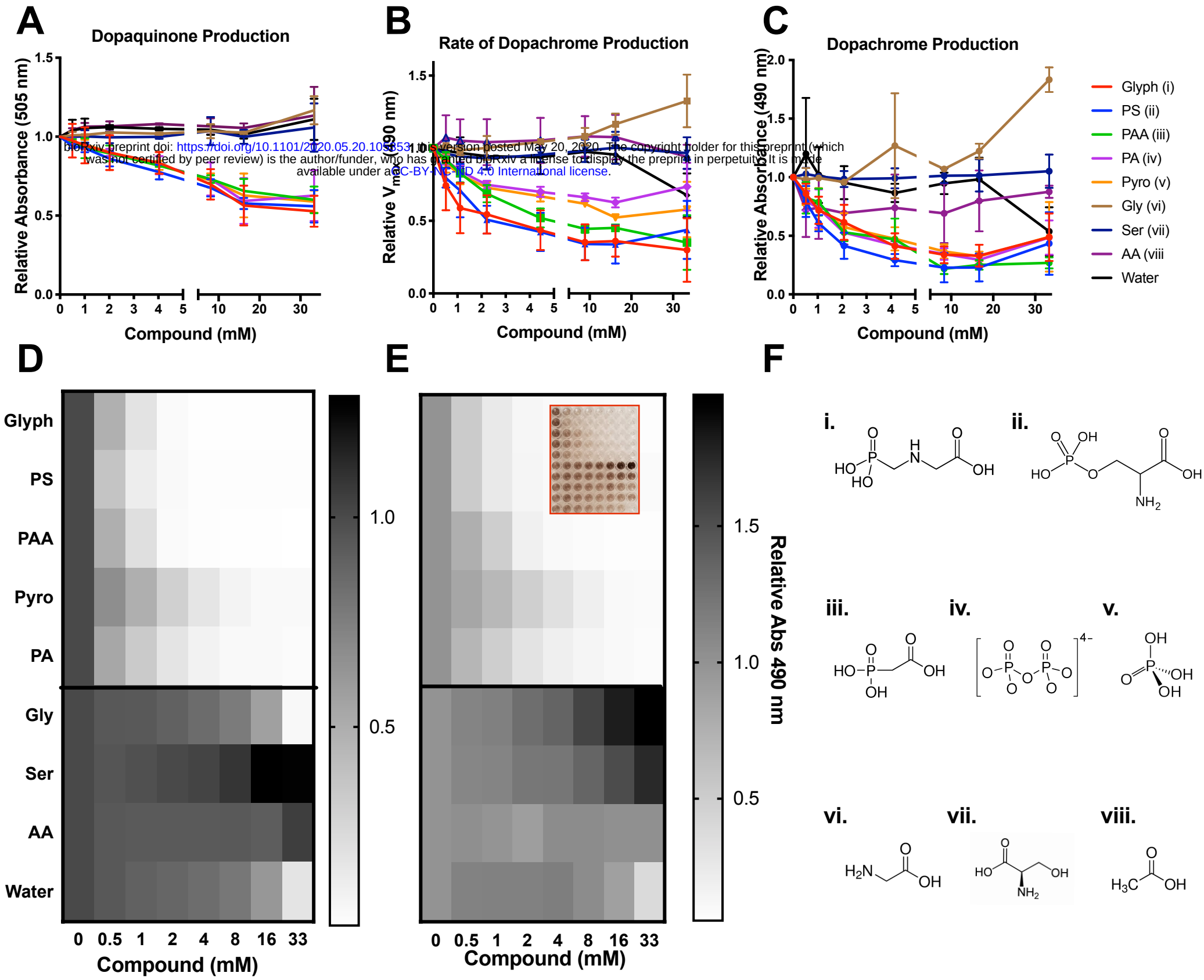

Fig. 2. ***Phosphate-Containing Compounds Inhibited Melanization Similarly to GLYPH.*** GLYPH, *o*-phosphoserine (PS), phosphonoacetic acid (PAA), pyrophosphate (pyro), and phosphoric acid (PA) inhibit DQ formation **(A)**, rate of DC formation **(B)** and DC levels **(C)**, and melanin formation **(D)**, whereas their respective non-phosphate analogs, glycine (gly), serine (ser), and acetic acid (AA) do not inhibit any step of melanization **(A-D)**. (**E)** Auto-oxidation of L-DOPA is inhibited by GLYPH, PS, PAA, Pyro, and PA in a similar manner. The compounds tested (**F)** were diluted in 300 mM stock solution and titrated to pH between 5 and 6. Absorption and rates are shown relative to the internal no drug control. Grayscale bars represent mean absorbance at 490 nm relative to no compound control. Error bars represent ±SD. Each experiment represents at least three independent replicates.

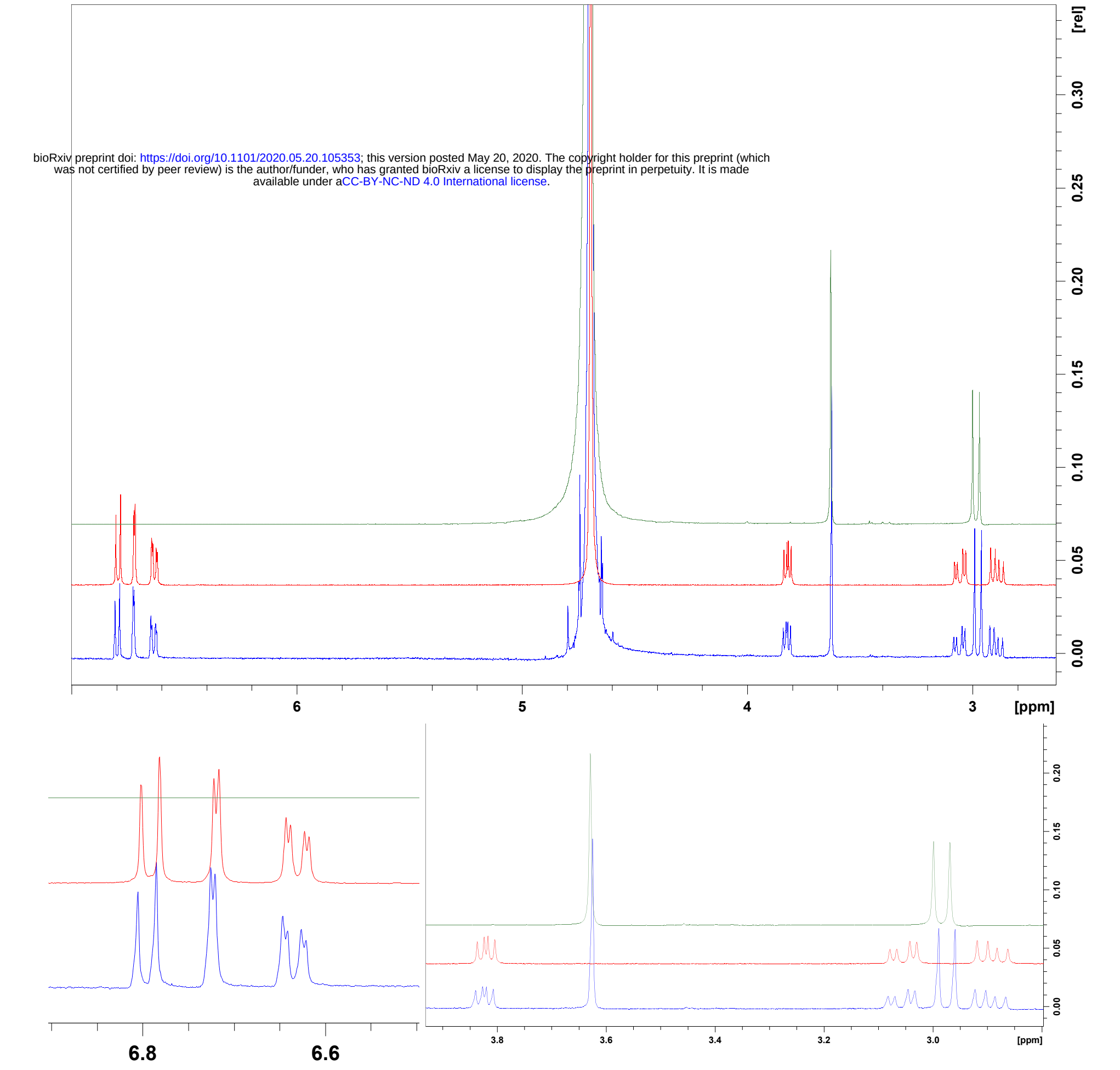

Fig. S1. ***Reaction of GLYPH with L-DOPA.*** Representative ^{1}H NMR spectra of 60 mM GLYPH solution in D_2O (**Green**), 20 mM L-DOPA solution in D_2O (**Red)**, and 20 mM L-DOPA mixed with 60 mM GLYPH in D_2O (**Blue**). There appears to be no shift in ^{1}H peaks and no appearance of new peaks, which is indicative of no reaction occurring between the compounds. Data representative of three independent replicates.

production (Fig. 3b). We treated different concentrations of tyrosinase with constant L-DOPA and GLYPH. There was a stable percent inhibition independent of tyrosinase concentration (Fig. 3c). This indicates that inhibition is not directly due to effects on the enzyme, but rather the reaction conditions. If GLYPH inhibited tyrosinase, we would expect a fixed difference between the activities of the GLYPH and control groups, which would result in parallel slopes in enzyme concentration vs. activity, leading to a decreased percent inhibition as the tyrosinase concentration increases.

Copper ions are important for tyrosinase activity. Since GLYPH is a metal chelator (Glass, 1984; Madsen et al., 1978), we evaluated whether GLYPH's effect was due to this property. We added copper ions to an L-DOPA and tyrosinase reaction to attempt to rescue the GLYPH inhibition. We performed the experiment with eight concentrations of copper (II) sulfate for each of the eight glyphosate concentrations. The addition of copper did not rescue the GLYPH dependent inhibition of melanin (Fig. 3d).

Interestingly, low concentrations of copper (6.25 - 25 μM) increased tyrosinase activity while high concentrations of copper (50 - 400 μM) reduced activity, indicating low copper can boost enzyme activity, while higher concentrations inhibit the reaction. However, this bimodal effect was not observed at increasing GLYPH concentrations (Fig. S2).

GLYPH Affects the Oxidative Properties of Melanogenesis

Melanogenesis is dependent on the spontaneous radicalization of quinone intermediates (Riley, 1988). DQ radicals and cyclodopa undergo a radical-mediated redox exchange that converts cyclodopa into DC and DQ into L-DOPA. Further downstream, ROS catalyze the polymerization of DHI into eumelanin. GLYPH's inhibitory effect could be due to a role as a free-radical scavenger or antioxidant. Since the inhibitory compounds blocked spontaneous oxidation of L-DOPA (Fig. 3e), they are "antioxidants". To measure this radical-quenching ability we used an ABTS assay in which ABTS radicals are blue, but when quenched the solution becomes colorless. The degree of discoloration is a proxy for radical concentration and antioxidant strength. GLYPH quenched the ABTS radical to some degree, but only after several hours of reaction (Fig. S3a), which did not occur with the other inhibitory phosphate-group containing compounds evaluated (Fig. 4a). This indicates that direct free-radical scavenging may not be the primary mechanism of melanin inhibition for GLYPH.

Phosphoric acid is a well-known synergist that boosts the antioxidant properties of phenolic compounds. Phosphoric acid, and other synergists such as citric acid, malic acid, and tartaric acid do not directly quench free radicals themselves, but instead work by regenerating

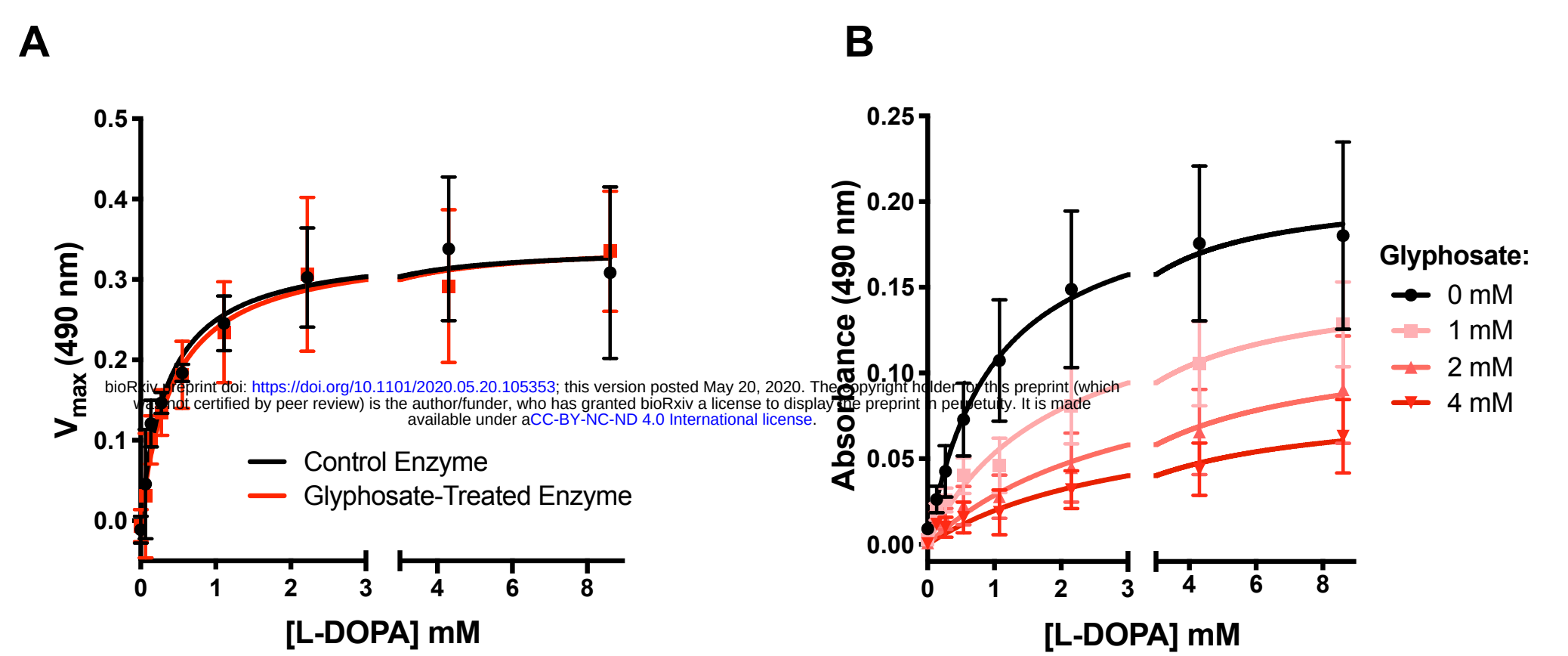

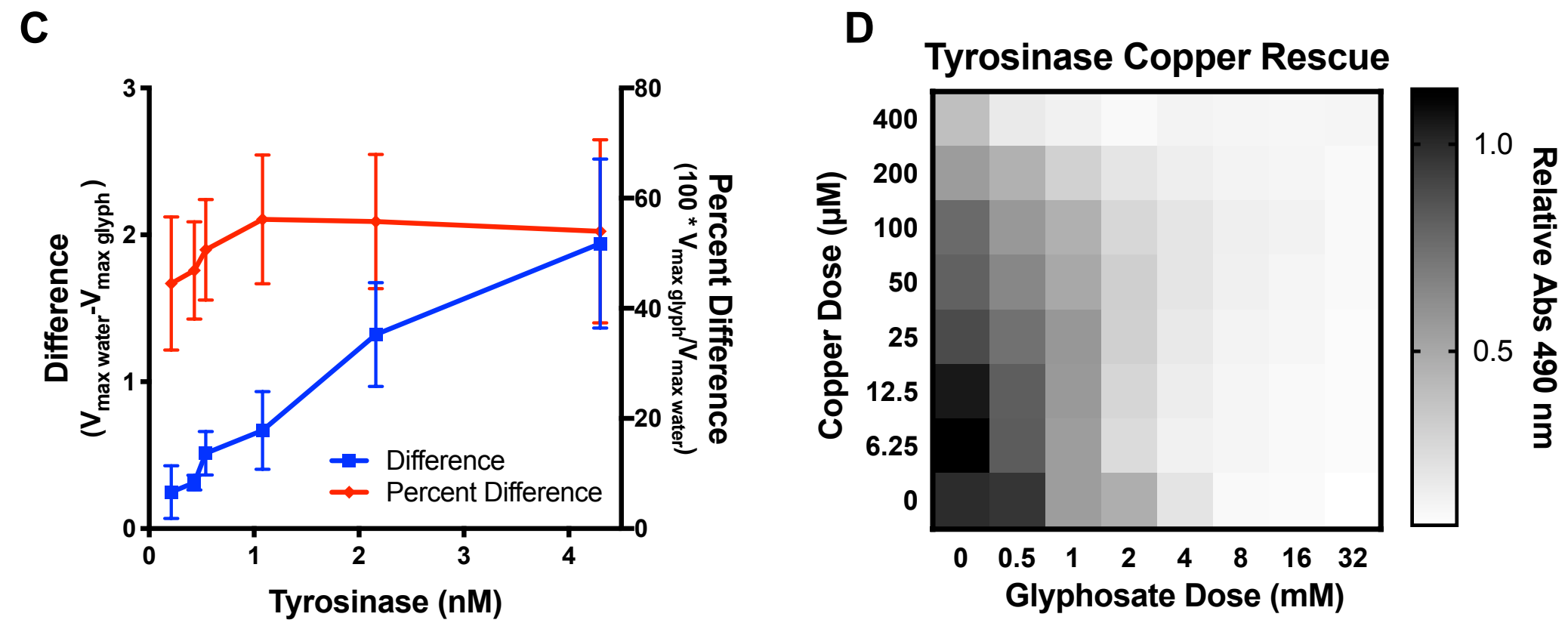

Fig. 3. ***GLYPH Does Not Directly Inhibit Tyrosinase Activity*** **(A).** Tyrosinase activity is not irreversibly inhibited and GLYPH-treated enzyme has normal activity when GLYPH is dialyzed out of solution. **(B)**. GLYPH appears as a non-competitive inhibitor of tyrosinase in Michaelis-Menten kinetics assays measuring the change in absorbance at 490 nm over 24 h compared to the no tyrosinase background. **(C)** The percent inhibition of DC formation rate with all GLYPH treatment remains constant over varying enzyme concentrations. The assay is performed under constant L-DOPA and GLYPH concentrations. **(D)** Adding Cu^{+2} to L-DOPA-tyrosinase reactions with GLYPH does not rescue melanin inhibition compared to the GLYPH-free control. (See also Fig. S2) Grayscale bars represent mean absorbance at 490 nm relative to no GLYPH and no copper control. Error bars represent ±SD. Each experiment represents at least three independent replicates.

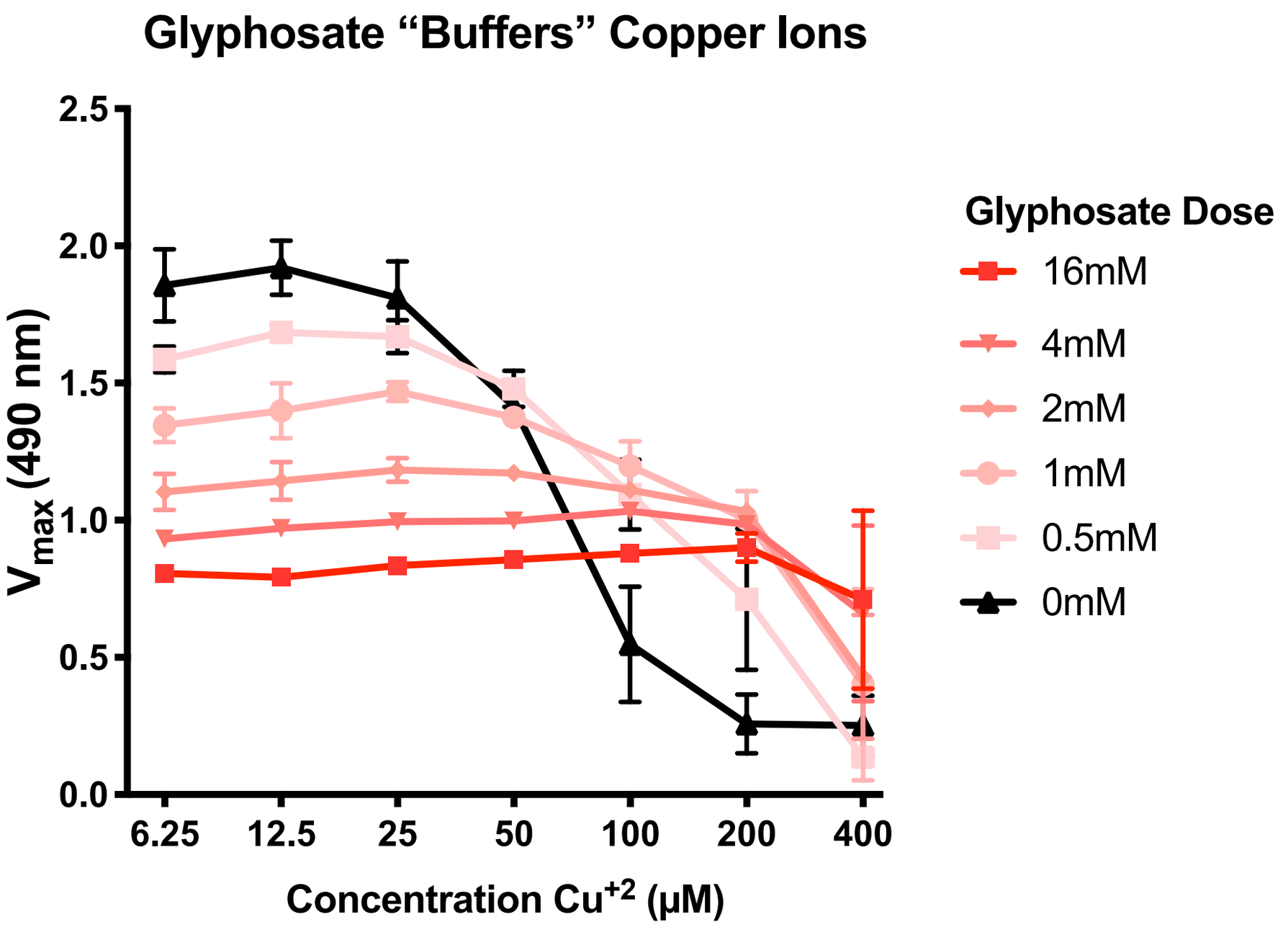

Fig. S2. ***GLYPH appears to "buffer" copper concentration in solution*****.** High doses (2-16 mM) of GLYPH prevent the enzymatic activity enhancing effects of lower copper concentration (6.25-25 μM), but high doses of GLYPH also prevent the enzyme inhibitory effects of high copper concentration (100-400 μM)**.** Error bars represent ±SD. Data represents at least three independent replicates.

antioxidants, becoming “sacrificially oxidized”, or chelating metal ions in solution (Gordon, 1990; Choe and Min, 2009). GLYPH could be reacting with existing antioxidants to strengthen and/or regenerate them into “active” form. In this instance, the GLYPH is bolstering the antioxidant properties of L-DOPA.

We observed that the synergist citric acid inhibited melanization similarly to GLYPH and phosphoric acid (Fig. 4b,c). The addition of GLYPH, phosphoserine, and phosphoric acid enhanced the antioxidant properties of L-DOPA in an ABTS assay in a similar manner as citric acid (Fig. 4d). This suggests that GLYPH may act as an inhibitor via synergism. The synergy is the ratio of the quenching capacity of the L-DOPA and the compounds alone to the quenching capacity of L-DOPA combined with the compound. The lower this ratio, the more synergistic the compounds are with L-DOPA (Fig. S3b). These values indicate that the inhibitory compounds are synergistic, whereas the non-inhibitory glycine and serine are not as synergistic.

The inhibition of melanin was independent of the L-DOPA to GLYPH ratio, and GLYPH’s IC_{50} is ~1 mM regardless of L-DOPA concentration (Fig. S4). This could be explained by a general antioxidant effect on solution.

GLYPH Alters the Oxidation-Reduction Potential of the System

L-DOPA is a more effective antioxidant when it is oxidized or radicalized, and has a better ability to form adducts with other radicals. Since GLYPH is acting as a synergistic antioxidant, it may be driving L-DOPA oxidation and possibly radicalization in which L-DOPA scavenges radicals better. This has the potential to disrupt melanin synthesis by stopping the spontaneity of redox exchange and DQ formation.

To investigate whether the addition of GLYPH changed the oxidation properties of L-DOPA, we used cyclic voltammetry – a technique to measure the electrochemical properties of solutions and previously used to study quinone electrochemistry (Bailey and Ritchie, 1985; Kissinger and Heineman, 1983). Voltammetry performed on L-DOPA solutions with GLYPH showed dose dependent shifts towards a negative potential (Fig. 4e,h) in peaks that corresponded to L-DOPA oxidation (Liu et al., 2003) (**Peak 1**). We validated these as L-DOPA oxidation peaks by performing voltammetry on various L-DOPA concentration **(data not shown**). The peak shift towards negative potentials indicates the L-DOPA was oxidized more easily and had less ability to be an oxidant, similar to the negative potential shifts associated with alkaline pH and increased oxidation (Fotouhi et al., 2009). We controlled for any pH-dependent peak shifts by adjusting each solution to pH 6.00 prior to measurement. Decreased

A

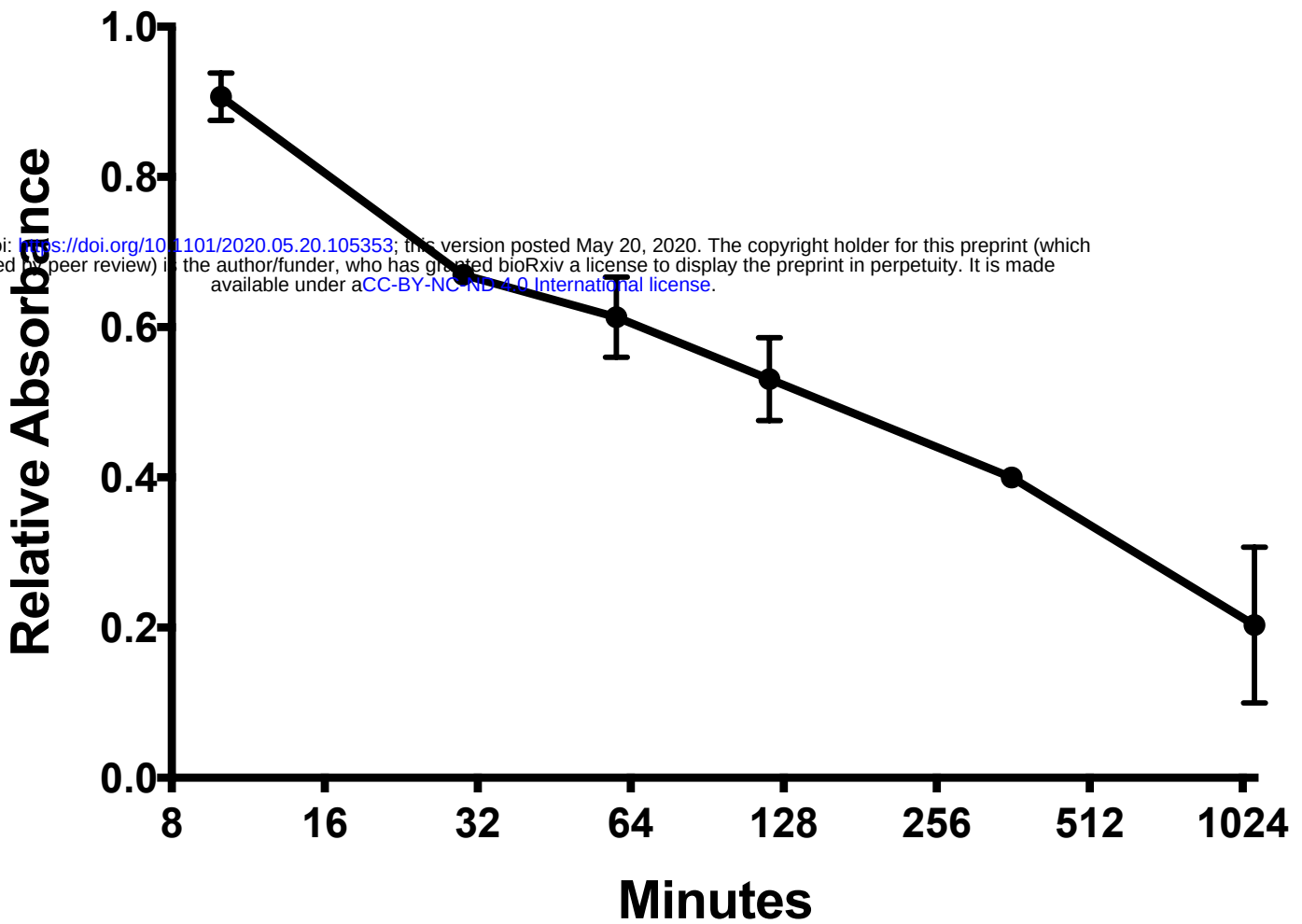

B

Compound	% Radical Quench- Compound Alone	% Radical Quench- Compound and L-DOPA	Synergy (Compared with L-DOPA alone)
Phosphoacetic Acid	0.020	72.288	0.483
Citric Acid	1.755	72.320	0.507
Phosphoric Acid	1.096	70.831	0.508
Pyrophosphate	3.320	72.675	0.526
Acetic Acid	1.327	64.155	0.565
Glyphosate	5.839	69.483	0.586
Phosphoserine	1.558	57.443	0.635
Glycine	-0.566	44.252	0.776
Serine	-0.386	40.808	0.846
Water	0.000	36.635	0.953
L-DOPA		**34.904**	**1.000**

Fig. S3. ***Antioxidant Properties of GLYPH.*** **(A)** Change in absorbance of ABTS solution at 734 nm over time for 33.33 mM GLYPH relative to the no GLYPH control. This indicates GLYPH quenches free radicals over an extended period of time. **(B**) Calculated antioxidant radical scavenging synergy between compounds tested and L-DOPA. Values represent the mean of at least three independent replicates. Error bars represent ±SD.

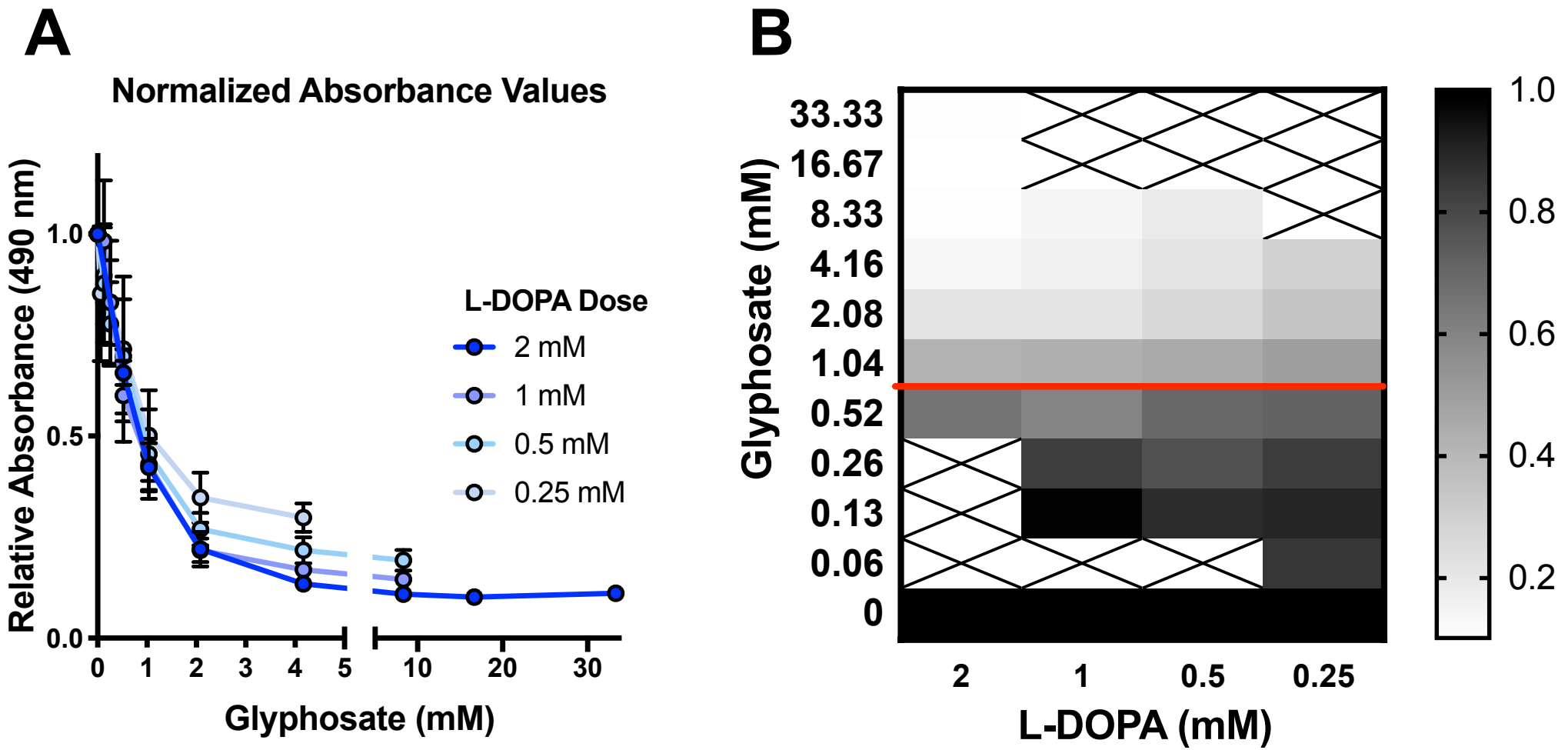

Fig. S4. ***GLYPH inhibits melanin production independent of L-DOPA concentration.*** (**A)** Inhibitory concentrations of GLYPH are not affected by L-DOPA concentration. This indicates that GLYPH is not reacting proportionately with L-DOPA as measured by absorbance at 490 nm after 5 d of reaction, relative to the no GLYPH control and with background absorbance subtracted. (**B**) The IC_{50} of GLYPH remains constant at approximately 1 mM relative inhibition of melanin production appears dependent on GLYPH concentration alone, and not on L-DOPA to GLYPH ratio. Error bars represent ±SD. Each experiment represents at least three independent replicates. Grayscale bars represent absorbance at 490 nm relative to no GLYPH control. Red line represents the approximate IC_{50}. Crossed out boxes represent values with no data.

oxidizing power can lead to significant effects, as melanin biosynthesis is reliant upon catechol oxidation and high redox potentials of quinones.

Interestingly, with increased GLYPH, the L-DOPA solution had a lower current intensity associated with the reduction of DQ to L-DOPA (**Peak 2)**. In cyclic voltammetry, smaller peaks indicate that less of the compound is oxidized or reduced. The decreased **Peak 2** current became virtually non-existent with increasing GLYPH concentrations (Fig. 4e,h,i). This implies that DQ, represented by **Peak 2**, is either not being formed during L-DOPA oxidation or cannot be reduced back into L-DOPA. These data indicate that the redox cycling steps of melanization are halted due to the inability of DQ to be reduced into L-DOPA. This could also indicate that while L-DOPA was oxidized more in the presence of GLYPH, it may form a non-DQ product - either a radical-mediated dimer with itself or a semiquinone.

GLYPH Inhibits Activity of *Galleria mellonella* and *Anopheles gambiae* Melanin-Producing Enzymes

In insects, POs are activated by serine proteases upon wounding or infection, thus triggering melanin production to either clot a wound or restrict a pathogen. The PO reaction is similar to the mushroom tyrosinase reaction in previous experiments. To investigate whether GLYPH inhibited insect melanogenesis, we used two models: *G. mellonella* wax moth larvae, and *A. gambiae* mosquitoes, a main vector of human malaria.

In an *ex vivo* analysis using *G. mellonella* hemolymph, we found that GLYPH inhibited PO activity in a dose dependent manner, without addition of exogenous substrate. Similar results were found with addition of a protease inhibitor, which was used to control for continued activation of PO, GLYPH-induced cellular responses, and/or off-target effects on other components of the PO cascade (Fig. S5a). GLYPH did not impact hemocyte viability (Fig. S5c). As seen with *Galleria*, GLYPH inhibited PO activity in whole-insect *A. gambiae* homogenate in a dose dependent manner. (Fig. 6a). These data show that GLYPH can inhibit melanization similarly in insects as it does in fungi, thus interfering with major melanin-based processes in at least two kingdoms of life.

We further tested if aminomethylphosphonic acid (AMPA), a primary breakdown product of GLYPH that accumulates in the environment (Sviridov, 2015), inhibits melanization similarly to GLYPH. Using *G. mellonella* hemolymph and mushroom tyrosinase, we found that AMPA inhibits melanization in both systems similar as GLYPH (Fig. 5 c,d).

GLYPH Alters the *G. mellonella* Susceptibility to Infection

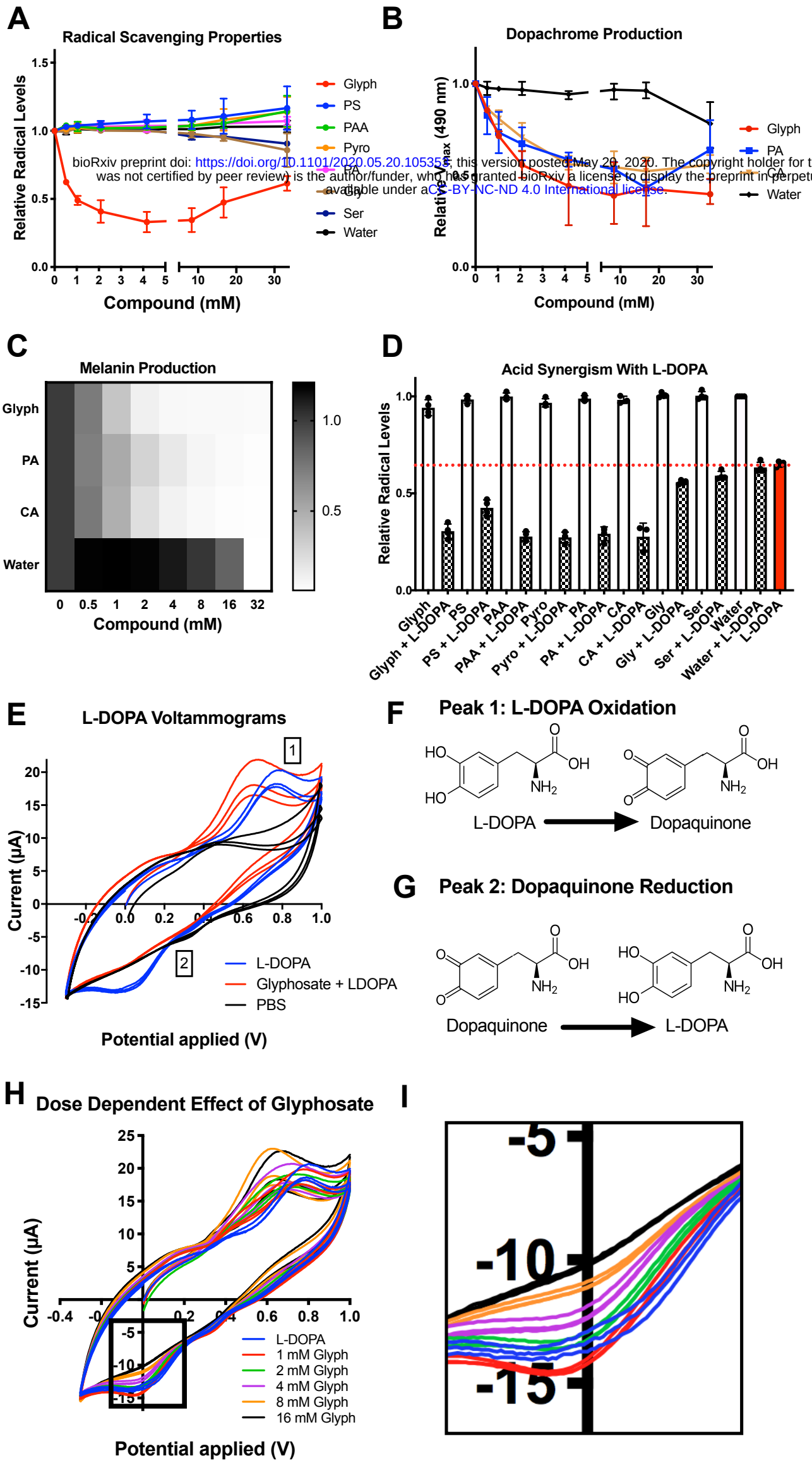

Fig. 4. *GLYPH Affects the Oxidative Properties of Melanogenesis.* (**A**) None of the melanin inhibitors exhibit radical quenching properties in an ABTS assay aside from GLYPH, which shows weak antioxidant properties after several hours in the ABTS solution. Absorbance at 734 nm is an indicator of how much ABTS remains in radical form (not quenched). (**B-C**) Citric acid (CA), a non-radical quenching antioxidant (antioxidant synergist) exhibits similar melanin inhibition as GLYPH and phosphoric acid, another known antioxidant synergist. **(D)** GLYPH, phosphoserine, phosphoric acid, and citric acid show synergy with the antioxidant L-DOPA. The addition of these compounds to L-DOPA enhances its radical quenching abilities by approximately 50%. Black dotted line represents the normalized ABTS absorbance treated with water. The other compounds tested here alone do not show much deviation from this line. The blue dotted line indicates the ABTS solution treated with L-DOPA alone. ABTS treated with L-DOPA and synergetic compounds together are below this line. (**E**) Average cyclic voltagram showing the changes in oxidation and reduction of L-DOPA and DQ when exposed to 16 mM GLYPH but not water. Numbers correspond to shifted peaks or peaks with less current compared to the water control. Peak 1 corresponds to L-DOPA oxidation (**F**); Peak 2 likely corresponds to DQ reduction (**G**). GLYPH shifts Peak 1 and 2 toward a decreased redox potential and diminishes the current of Peak 1 and 2 in a dose-dependent manner (**H**) - notably decreasing Peak 2 current intensity to the point of non-existence **(I)**. Grayscale bars represent absorbance at 490 nm relative to no compound control. Error bars represent ±SD. Each experiment represents at least three independent replicates. See also Fig. S3 and Supplemental Information.

Next, we sought to determine whether GLYPH increases *in vivo* susceptibility of insects to foreign organisms. We injected *G. mellonella* larvae with 2 µg of GLYPH (~8-12 ng/mg per larvae) followed by infection with *C. neoformans* or a mock infection. The two mock infected groups (GLYPH-treated and PBS-treated) exhibited similar survival. However in the infected groups, the GLYPH-treated larvae died faster compared to the PBS-treated controls (Fig. 5d). A similar, but non-significant, trend was seen in the infections with *C. neoformans lac1Δ* strain (Fig. S6d). The *lac1Δ* strain is unable to produce melanin, which is an important virulence factor in *C. neoformans* pathogenesis. The *lac1Δ* is less virulent in *G. mellonella* models (Mylonakis et al., 2005), potentially contributing to the lack of significant differences between the GLYPH and PBS treated groups**.**

GLYPH Alters *A. gambiae* Susceptibility to Infection and Survival

To investigate whether GLYPH renders mosquitoes more susceptible to infection with the human malaria parasite *P. falciparum*, adult female mosquitoes were fed GLYPH for 5 days and then given a *P. falciparum*-infected blood meal. GLYPH-fed mosquitoes had higher median parasite burden, measured as oocysts per midgut (Fig. 6c). Overall, oocyst burden increased with increasing dose of GLYPH. However, we observed a significant decline in parasite burden in the 10 mM treated group, which may have been due to high death rate of this group (Fig. 6b) resulting in few surviving mosquitoes to assess the intensity of infection. We also found that infection prevalence was higher in mosquitoes fed with 300 µM and 1 mM GLYPH, but did not reach statistical significance (Fig. 6d). In a low *P. falciparum* infection replicate (Fig. S6), we observed that GLYPH-treated groups are more likely to be infected than control groups. This is important, as lower burdens are reminiscent of the infections in malaria endemic regions (Gouagna et al., 1998; Sinden and Billingsley, 2001; Smith et al., 2014; Whitten et al., 2006).

Lastly, sugar preparations with GLYPH at environmentally relevant concentrations were given to *A. gambiae* mosquitoes to ascertain the herbicide's effect on the mosquito's lifespan. Compared to control mosquitoes (sugar-fed without GLYPH), mosquitoes given low drug doses (100 µM to 1 mM) showed improved survival, while those fed higher doses of GLYPH (3 mM to 10 mM) had equal or worse survival. (Fig. 6b). This suggests that GLYPH could have bimodal effects on mosquito health.

GLYPH Alters the Composition, but Not Density, of the *A. gambiae* Midgut Microbiome

A. gambiae midgut microbiome has been implicated in modulating anti-*Plasmodium* responses (Bahia et al., 2014; Bai et al., 2019; Dong et al., 2009; Romoli and Gendrin, 2018).

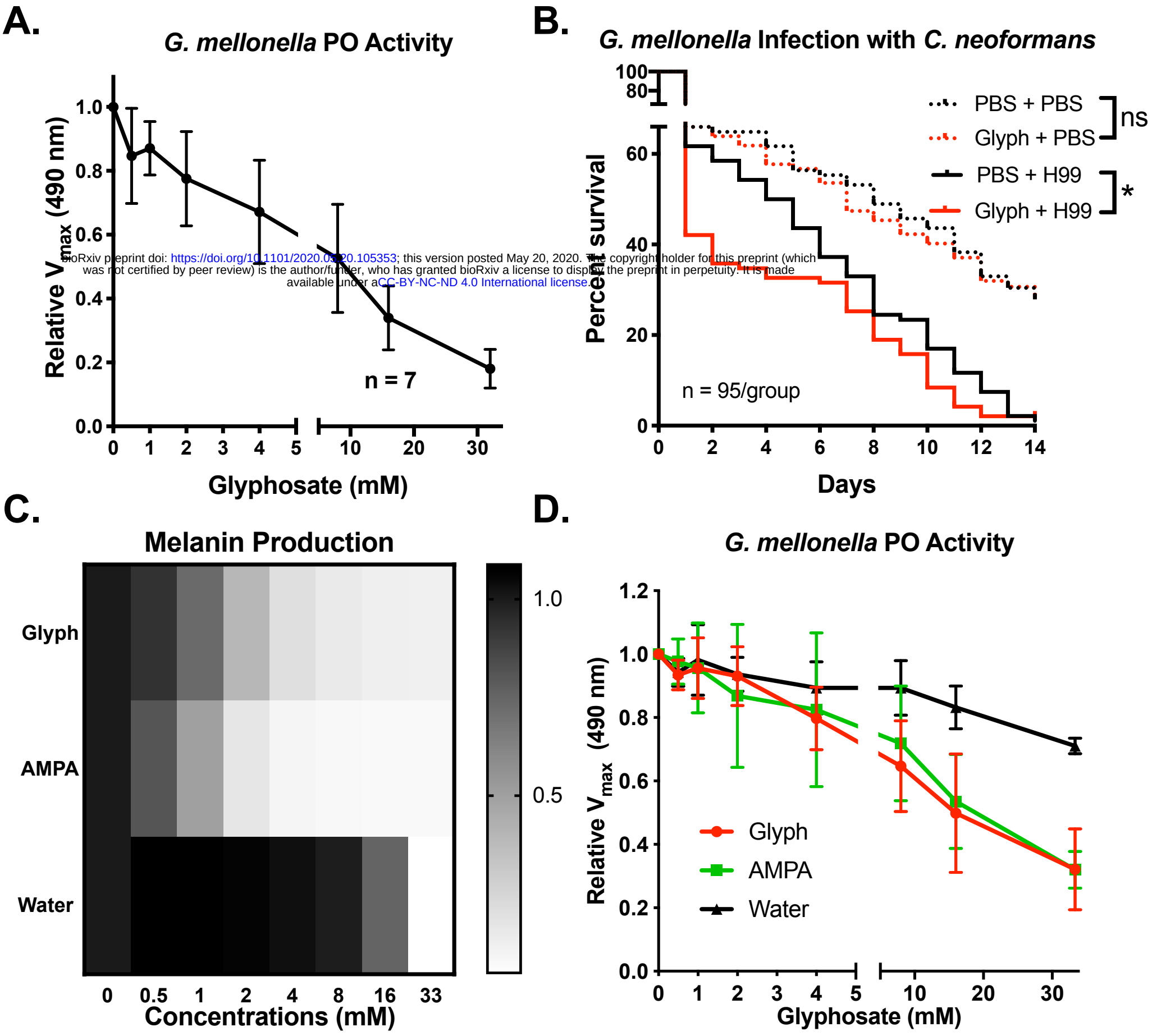

Fig. 5. ***GLYPH Inhibits G. mellonella Melanization and Increases Infection Susceptibility.*** (**A**) GLYPH inhibits the PO activity of 1:10 dilutions of hemolymph without exogenously added L-DOPA. (**B**). *G. mellonella* larvae drugged with GLYPH solution in PBS and infected 5 h post treatment with 10^4 cells of WT *C. neoformans* die rapidly compared to PBS-treated controls. Death events were recorded daily. AMPA, a primary metabolite of GLYPH, inhibits tyrosinase-mediated (**C**) and *G. mellonella* PO-mediated melanization similar to GLYPH. Error bars represent ±SD. Each infection condition represents survival of 95 animals, over the span of four biological replicates, and six total technical replicates. See also, Fig. S5.

Fig. S5. *G. mellonella* Supplemental Data. (A) Protease inhibitor is added to *G. mellonella* hemolymph to prevent the activation of new phenol oxidase, and to control for any impact that GLYPH may have on phenol oxidase activation cascade, cell viability, and gene expression. The general trend remains the same that GLYPH inhibits phenol oxidase activity with and without protease inhibitor, albeit lower with protease inhibitor due to the lower concentration of activated enzyme. **(B)** PO activity was assessed using exogenous L-DOPA for one batch of *G. mellonella,* during these experiments, the lower concentration of GLYPH resulted in increased PO activity as compared to the control. This suggests that there may be some cellular regulation of PO induced by GLYPH. It is possible that the doses of GLYPH tested elicit some cellular response that increases PO expression, secretion, and/or activation as a feedback response to the reduced melanin production. These data represent three independent replicates, but this pattern of enzymatic activity as a function of GLYPH concentration was not seen in subsequent batches of larvae. (**C)** Hemocyte viability was not dramatically affected by concentrations of GLYPH ranging from 100 µM to 10 mM, indicating that our data are likely not artifacts of cytotoxic concentrations of GLYPH. **(D)** Larvae treated with GLYPH and subsequently infected with *lac1Δ* mutant *C. neoformans* strain showed a similar pattern of increased susceptibility as the wild type H99, although the differences in susceptibility with the *lac1Δ* infected larvae are not statistically significant. Error bars represent ±SD. Each experiment represents at least three independent replicates. The PBS mock infection condition represents survival of 95 animals, over the span of four biological replicates, and six total technical replicates. The *lac1Δ* mutant infection represents survival of 75 animals over the span of four biological replicates. The PBS mock infection data is the same as the data in Fig. 5b, as all the infections were done concurrently under the same conditions.

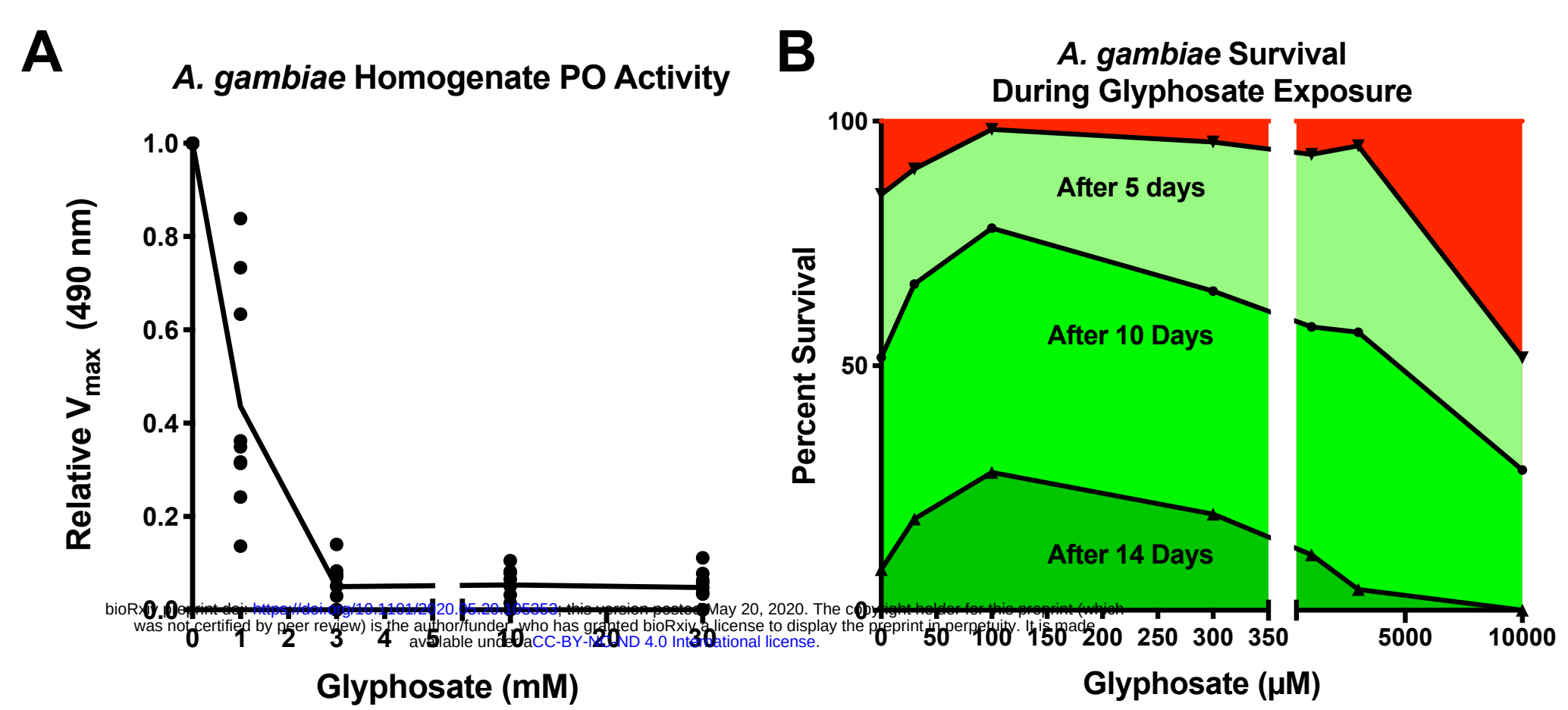

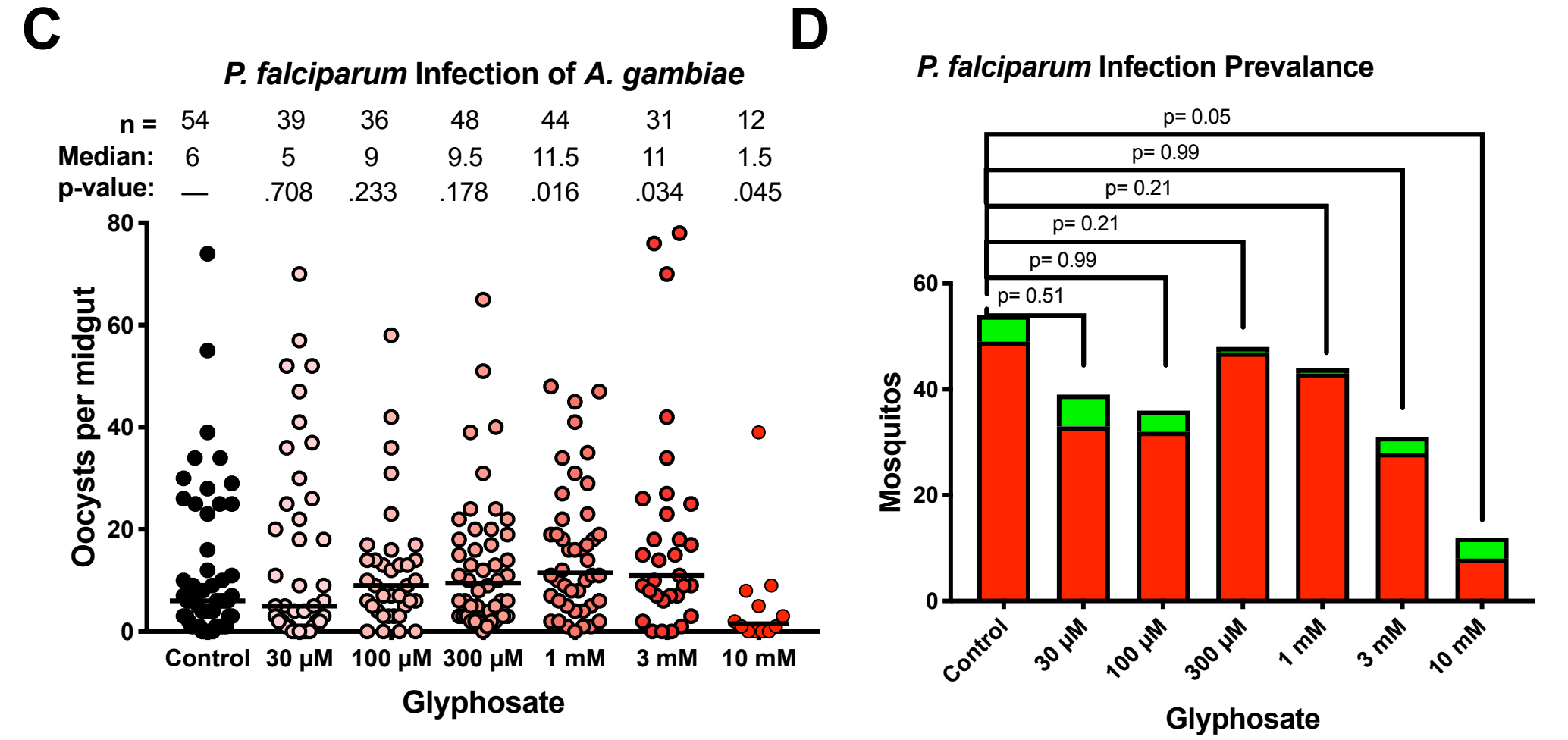

Fig. 6. ***GLYPH Effects on A. gambiae Immune System***. (**A**) GLYPH inhibits PO activity in *A. gambiae* homogenate. (**B**) Low doses of GLYPH enhance the survival of adult mosquitoes, while the higher doses diminish their survival as compared to the control. **(C)** GLYPH treatment increases the susceptibility of the *A. gambiae* to *P. falciparum* infection as measured by oocyst count per midgut. Increased GLYPH doses are associated with increased median oocyst burden. (**D**) There is not a significant difference in the *P. falciparum* infection prevalence between GLYPH-treated and untreated mosquitoes, however, there is a trend of increased infection prevalence in 300 µM and 1 mM GLYPH treatment groups. Enzyme activity represents three biological replicates with three technical replicates for each condition. Survival curves represent 120 animals, across three biological replicates. Parasite infection represents four biological replicates and four separate infections, line indicates median, and differences in parasite burden analyzed for significance using two-tailed non-parametric Mann-Whitney test with each group compared to the control group. Infection prevalence was analyzed for significance using Fischer's exact chi-squared test. See also Fig. S6.

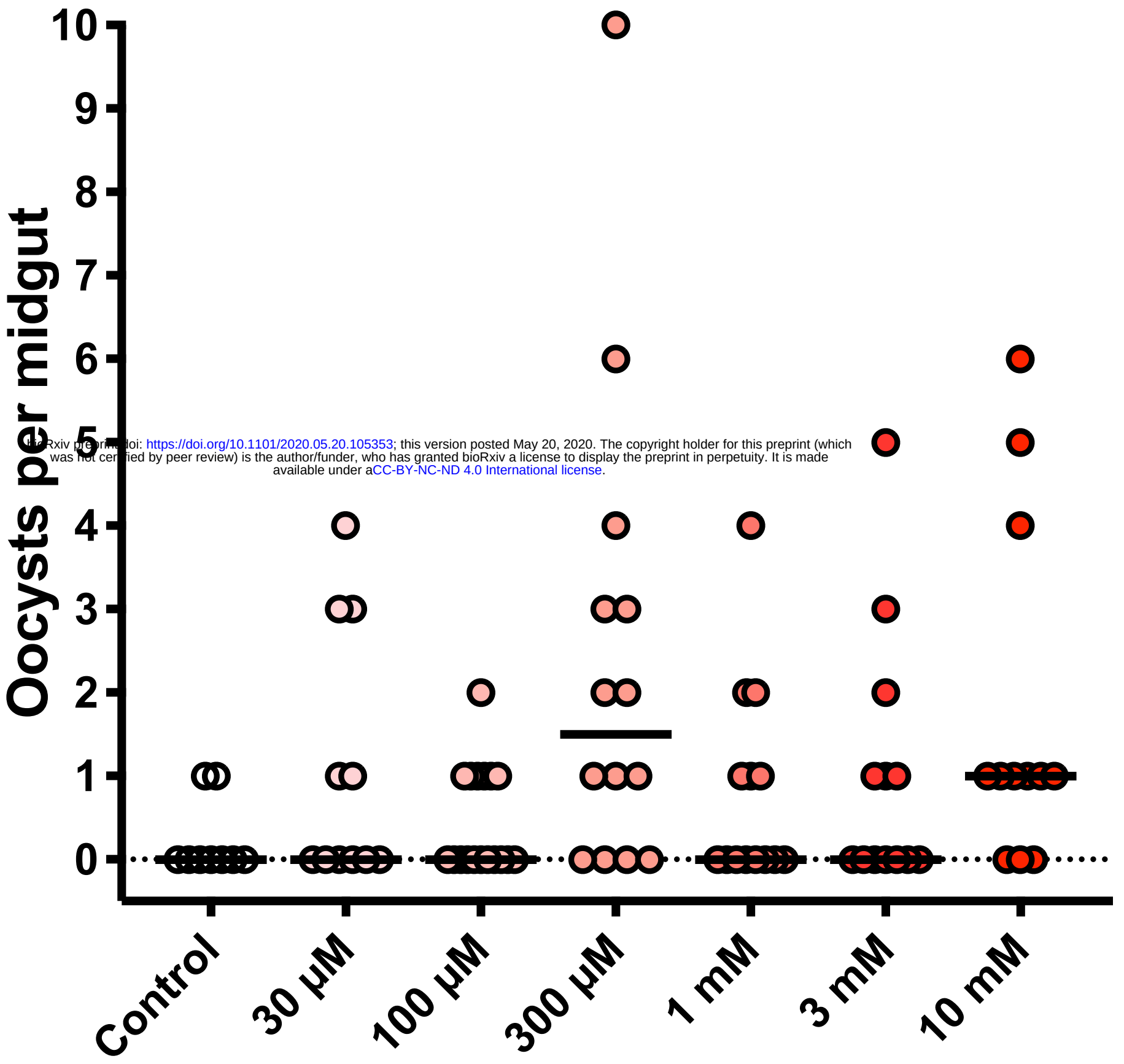

Fig. S6. Low efficiency *Plasmodium falciparum* infection of *A. gambiae* Oocyst count per midgut for mosquitoes treated with or without GLYPH and infected with high-passage *Plasmodium falciparum* gametocyte culture, resulting in a low efficiency infection. Data represents one biological replicate. Dotted black line indicates y=0. Black lines for each condition indicate median oocyst count per midgut. We have chosen not to include the data from this replicate in the data shown in Fig. 6, because the results from this one-off replicate appear due to poorly infectious parasite culture. Additionally, it is difficult to make comparisons using the low infection burden of the control group with a with the treatment groups, as well other replicates with higher oocyst burdens.

We investigated if GLYPH had detrimental effects on the *A. gambiae* microbiome. Colony Forming Unit (CFU) counts from cultures of midgut homogenates grown on LB agar demonstrated that GLYPH treatment did not affect gut bacterial density (Fig. 7a). However, 16S rRNA analysis of midgut microbiome indicates a shift in composition with GLYPH treatment. GLYPH treatment was associated with a decrease in the relative abundance of Enterobacteriaceae and an increase in relative *Asaia spp.* populations (Fig. 7b), but a dose-dependent impact on composition was not observed. Analysis indicates that the GLYPH treatments reduce the alpha diversity (Shannon Index) and may affect the diversity of the microbiome within populations (Fig. 7c). The microbiota of the GLYPH-treated groups and controls are dissimilar and form two separate clusters in principal coordinates analysis as measured by Bray-Curtis dissimilarity (Fig. 7d). These differences suggest a shift in beta diversity, and therefore a difference between the microbial communities of mosquitoes exposed to GLYPH versus untreated controls.

DISCUSSION

GLYPH use has caused concerns regarding its potential effects on human health, soil fertility, microbial ecosystems, and insect populations. In the present study, we investigated the effect of GLYPH on melanin production. We parsed through the mechanism by which GLYPH inhibits melanogenesis and show that it is due to effects on the oxidation-reduction potential of the catalytic reaction. Although GLYPH is a relatively weak inhibitor of melanization, the inhibitory concentration could be relevant in nature given the vast amounts used in agriculture, especially as its breakdown product AMPA was also active. We correlated GLYPH's effects on the insect melanin-based immune response and their pathogen susceptibility. We observed that GLYPH enhanced the susceptibility of two insects to infection. This raises concerns that GLYPH can interfere with invertebrate immunity through its effects on melanin-based defense mechanisms.

Many melanin inhibition mechanisms are known (Borovansky and Riley, 2011). An inhibitor could react with the substrates for tyrosinase or PO, such as L-DOPA, and prevent its conversion to the quinone product. A compound could directly block the substrate's access to the enzyme by binding to the active site or affecting the enzyme's conformation by allosteric binding. Similarly, compounds could chelate the copper ions necessary for the enzyme's catalytic core. Lastly, inhibitors could stabilize quinones, quench free radicals, or otherwise alter the redox potential of the system, thus preventing the proper spontaneous cascade and formation melanin.

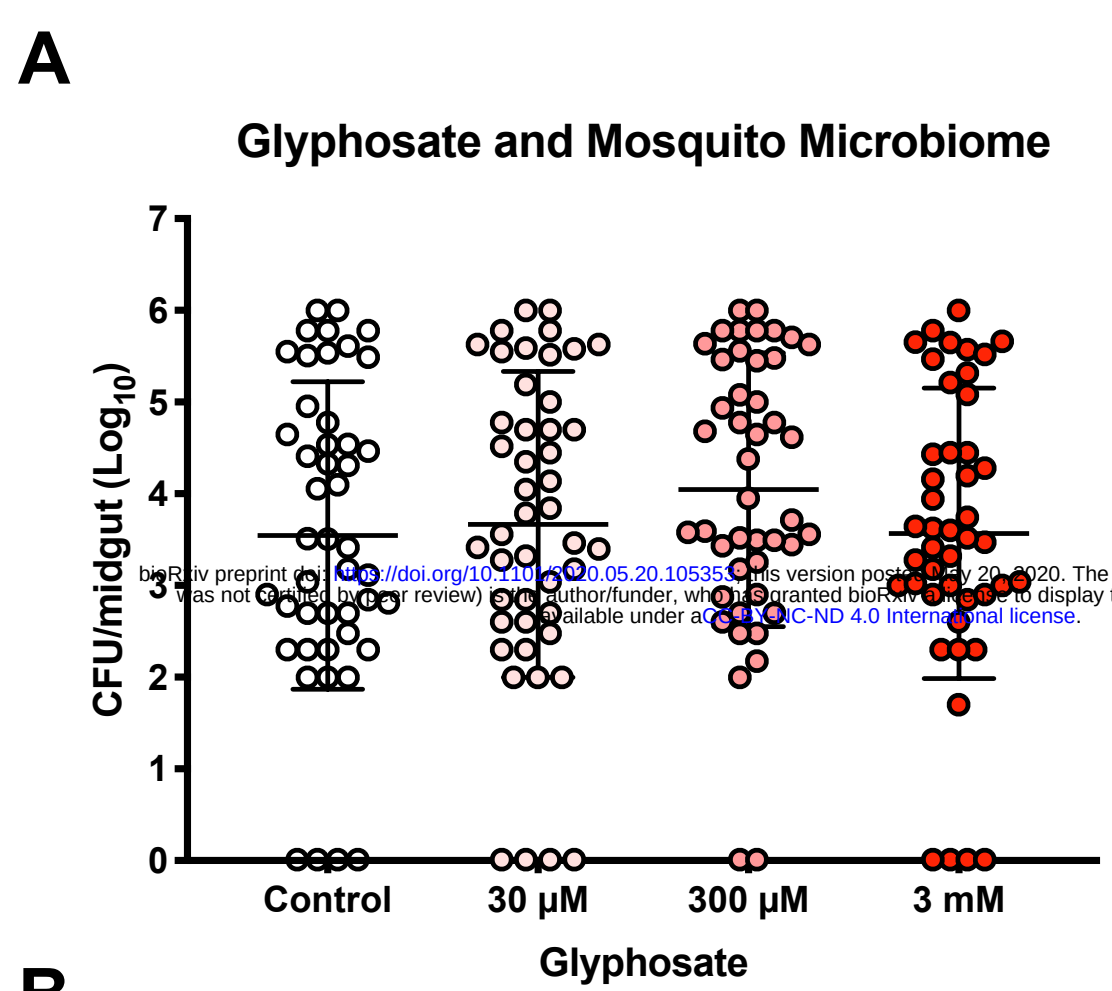

Fig. 7. GLYPH Alters the Composition, but Not Density, of the *A. gambiae* Midgut Microbiome. (**A)** GLYPH does not alter microbial density of the culturable mosquito midgut microbiome (grown on LB agar). Each sample consists of 40-50 individual mosquito midguts over three independent replicates. Error bars represent the mean and ±SD. **(B)** GLYPH alters the composition of the mosquito microbiota, leading to depletion of Entereobacteriacae and a bloom of *Asaia spp.* The GLYPH treatments are associated with a decrease in alpha diversity **(C),** and the GLYPH-treated and control-treated microbiota form distinct populations (**D**). Each treatment group represents 5 individual mosquito midguts. For more information see also Fig. S7.

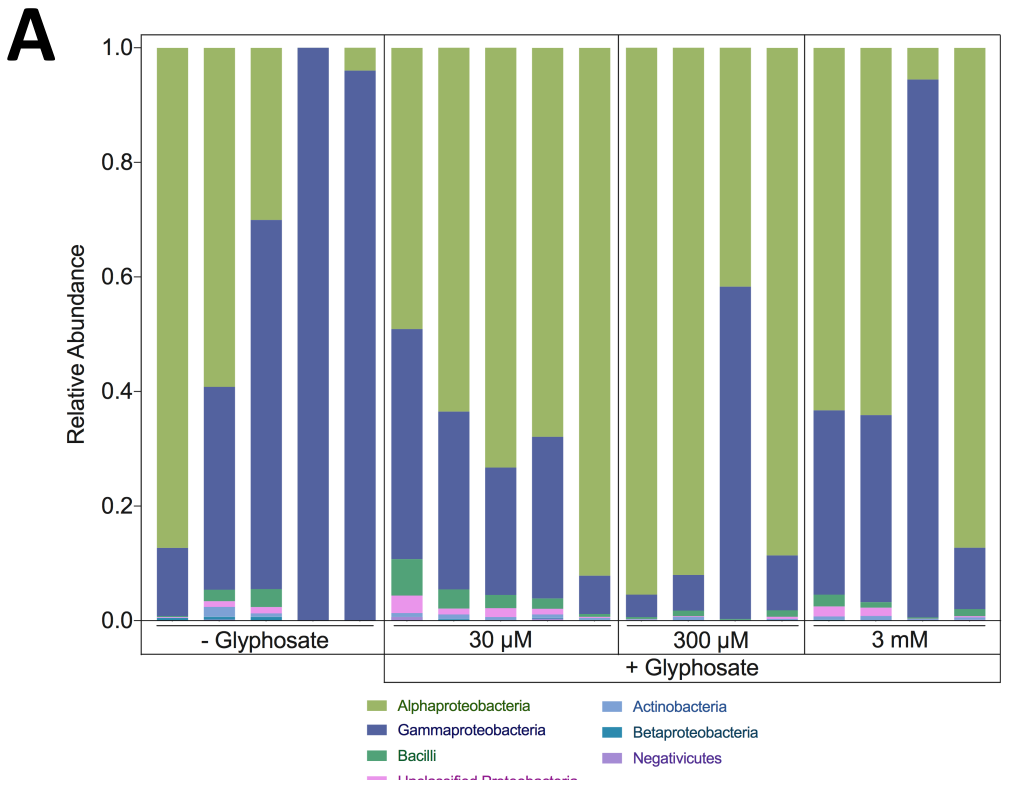

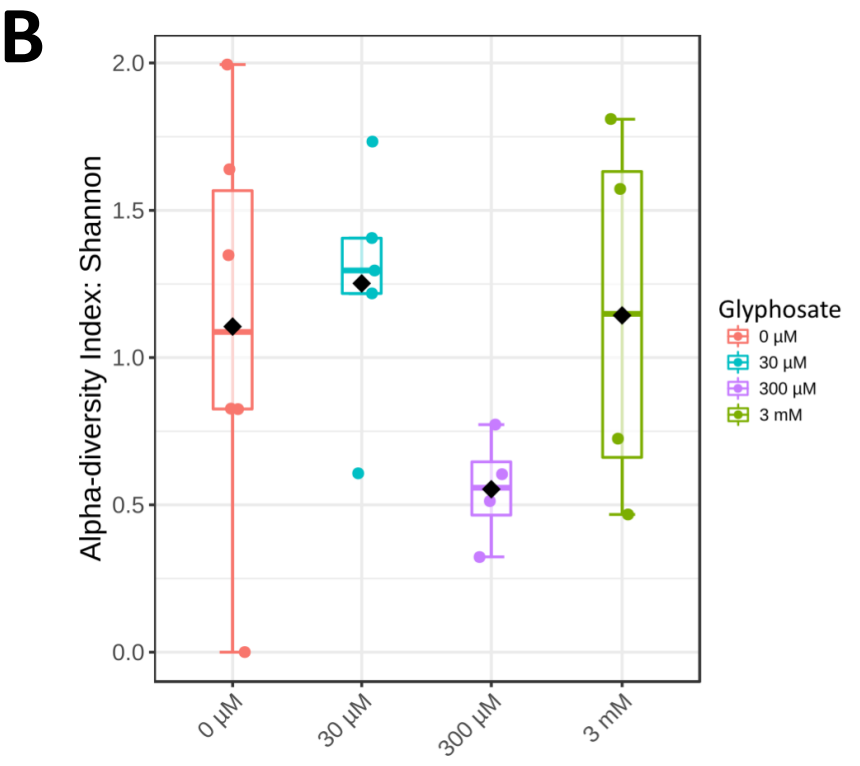

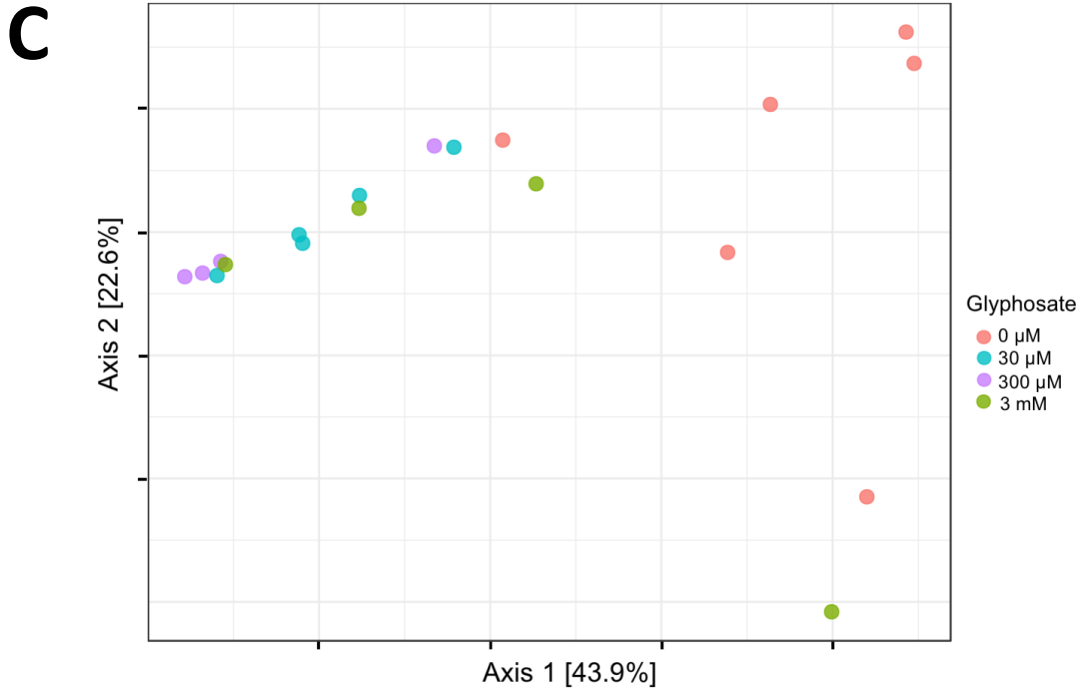

Figure S7: GLYPH affects the *A. gambiae* microbiome in a dose-independent manner (A) At the class level, GLYPH leads to an enrichment of Alphaproteobacteria and a depletion in Gammaproteobacteria. **(B)** Alpha diversity does not follow a distinctive pattern with increasing GLYPH dose. **(C)** GLYPH-treated and control-treated microbiota cluster separately in ordination space, but the clusters are not dose-dependent.

The first step in the melanin pathway is the conversion of L-DOPA into DQ through enzymatic or spontaneous oxidation of L-DOPA. GLYPH, as well as other phosphate-containing compounds such as phosphoserine, phosphoacetic acid, pyrophosphate, and phosphoric acid inhibited formation of DQ. Our results strongly suggest that these compounds inhibit the oxidation of L-DOPA itself in an enzyme independent manner. These compounds also inhibited the auto-oxidation of L-DOPA (Fig. 3e), further indicating that interference with melanin production is independent of tyrosinase. Furthermore, we found no evidence that GLYPH reduced tyrosinase activity in an irreversible manner (Fig. 2a).

Tyrosinase and PO require copper to catalyze the conversion of phenolic substrates into quinone products; while GLYPH is a copper chelator, adding back copper ions did not rescue the GLYPH-induced inhibition of melanin (Fig. 2d). Interestingly, low copper increased tyrosinase activity and high doses reduced activity when no GLYPH was present. However, with high concentrations of GLYPH, copper concentration had minimal effect on tyrosinase activity (Fig. S2). It appears that GLYPH, possibly through chelation, acts as a “buffer” of copper ions and can reduce the harmful effects of the metal on the enzyme. This could have implications for melanogenesis in nature, where some fungi such as *C. neoformans* use copper as a signal to upregulate the melanin-producing enzyme laccase. If copper ions are sequestered via GLYPH, it could reduce laccase expression and melanin production (Jiang et al., 2009), which could contribute to the GLYPH-based inhibition of melanin previously described in *C. neoformans* (Nosanchuk et al., 2001).

We examined the possibility that the inhibitors quench free radicals in solution, which are necessary for continuation of melanin production. Of the inhibitors tested, only GLYPH had radical-quenching activity, but it was relatively slow (Fig. S3a). Phosphoserine has a similar structure and near identical inhibition as GLYPH but no radical-quenching properties, this property is likely not the mechanism of inhibition. While the other phosphate containing compounds we tested did not quench free radicals (Fig. 4a), phosphoric acid is a known antioxidant synergist. Synergists enhance the antioxidant properties of phenolic compounds, some via chelating metals, and others by reverting antioxidants into their active states (Choe and Min, 2009). Synergists such as phosphoric acid, citric acid, malic acid, and alpha-hydroxy acids are added to foods, medicines, and cosmetics as preservatives due to synergistic properties, and used at concentrations up to 10% (Yu and Scott, 1982). In our system, we believe that GLYPH behaves similarly to phosphoric acid and citric acid. We observed that citric acid inhibited melanogenesis in a manner similar to GLYPH and phosphoric acid, suggesting an inhibition mechanism via antioxidant synergy. In addition, we report that GLYPH,

phosphoserine, and phosphoric acid have similar synergistic effects as citric acid when combined with L-DOPA in solution versus L-DOPA alone (Fig. 4d). This further shows that GLYPH is an antioxidant synergist. In order for L-DOPA to be an antioxidant, it must either be reduced back to a normal state from an oxidized state, or it must have a free radical and undergo an adduct reaction with another radical compound to form a new molecule. Since GLYPH is making L-DOPA a more efficient antioxidant, GLYPH alters the oxidative balance of L-DOPA, and/or causes a buildup of radical or semiquinone intermediates.

Melanin synthesis is dependent upon coupled redox cycling between quinones and catechols. If the oxidizing ability and the redox potential are altered, the ability of the process to proceed is also diminished. We used cyclic voltammetry to test GLYPH's interference with the redox status of L-DOPA solution. We found that GLYPH decreased the redox potential of L-DOPA-DQ (Fig 4e,h). This indicates the L-DOPA becomes a weaker oxidizing agent, stronger reducing agent (antioxidants), and thus more prone to oxidation. This is consistent with the antioxidant synergy seen in the ABTS assay. Further, addition of GLYPH dose-dependently decreased the DQ reduction current (**Peak 2**), indicating that DQ is not produced by the oxidation of L-DOPA, or DQ is unable to be reduced if it *is* produced. The lack of DQ could indicate that GLYPH causes L-DOPA to oxidize into a semiquinone or radical intermediate that does not form DQ. These intermediates could react with each other and form L-DOPA dimers or remain stable. Further, if DQ is unable to be reduced into L-DOPA, subsequent melanin biosynthesis becomes unfavorable as redox exchange could not occur. These changes in voltammogram do not appear when the L-DOPA solution is treated with 16 mM glycine, but do appear with citric acid (**data not shown**). This further supports that GLYPH is acting as an antioxidant and prevents the redox-dependent melanin biosynthesis.

GLYPH's disruption of biochemical processes is relevant to the health of the biosphere. Multiple studies have shown that GLYPH has negative effects on ecosystems by disturbing microbial populations and inducing oxidative stress in plants, rats, fish, amphibians, and insects (de Aguiar et al., 2016; El-Shenawy, 2009; Güngördü, 2013; Nwani et al., 2013; Uren Webster and Santos, 2015). This, interestingly, bolsters our findings that GLYPH promotes oxidation/radicalization in compounds like L-DOPA. Our results further demonstrate that GLYPH can inhibit melanization and PO activity in *G. mellonella* and *A. gambiae* (Figs. 5a, 6a), while increasing their susceptibility to foreign microbes (Figs 5b, 6c).

GLYPH makes *A. gambiae* more susceptible to parasite infection, however melanization is not considered this human malaria model's major anti-*P. falciparum* immune response. The increased susceptibility of *A. gambiae* to *P. falciparum* could be due to broader alterations of

mosquito immune defenses or to disruption of non-melanin roles of catecholamines and PO in insect immunity, such as cytotoxic intermediates and ROS (Nappi and Christensen, 2005; Urabe et al., 1994; Zhao et al., 2011). Importantly, we observed that even when mosquito infections resulted in an overall low parasite burden, GLYPH-treated groups exhibited a higher infection incidence and intensity than controls. This is notable because *Plasmodium* oocyte development within the mosquito is a major bottleneck to successful vector competence (Smith and Barillas-Mury, 2016) - if a mosquito can prevent oocyst formation, there is no transmission of malaria to humans. Our data may indicate that mosquitoes exposed to GLYPH are less able to control *Plasmodium* infection, thereby becoming better vectors for malaria. Conversely, after treatment with a high GLYPH concentration (10 mM) and infection with *P. falciparum* we noticed decreased susceptibility to the parasite (Fig. 6c). Intriguingly, this group also had the lowest survival by the end of drugging, blood feeding, and infection with *Plasmodium.* This points to an interesting effect, in which high concentrations of GLYPH reduce mosquito survival, but those that survive these high concentrations resist *P. falciparum* infection with greater success. Furthermore, our data revealed that lifespan of uninfected adult female mosquitoes was enhanced at low doses of glyphosate compared to the control. This greater longevity may be due in part to reduced basal damage from host defense mechanisms that normally occur during melanin formation, and/or altered gut microbiota. Hence, these longer-living-immunosuppressed mosquitoes are more susceptible to infection with *P. falciparum,* as a result, they are better vectors for transmitting malaria to humans. In contrast, mosquitoes exposed to high concentrations of GLYPH showed decreased survival but greater susceptibility to infection. These data open up the broader notion of whether GLYPH has multifaceted outcomes on vector competence.

Altogether, our results are consistent with reports that GLYPH makes honeybees more susceptible to infection, a finding attributed to gut microbiota perturbation and an effect on the microbial shikimate pathway (Motta et al., 2018). In this regard, our data suggest an additional explanation for these findings due to inhibition of melanogenesis - a critical part of insect immune defense. These mechanisms of susceptibility are not mutually exclusive, and could be additive to weaken insect health. Importantly, our analyses of *A. gambiae* midgut microbiota indicated that GLYPH did not impact *A. gambiae* midgut bacterial density; however, the herbicide did perturb midgut microbiota composition in a non-dose dependent manner. More specifically, GLYPH reduced diversity of the microbial community - GLYPH-treated mosquitoes exhibited diminished Enterobacteriaceae and expanded *Asaia* spp populations. The presence of some Enterobacteriacae, including the common insectary contaminant *Serratia marcescens,* in

Anopheles spp. midgut are associated with lower susceptibility to *Plasmodium spp.* infection (Bando et al., 2013; Cirimotich et al., 2011). Depleting these bacteria with GLYPH exposure may result in increased susceptibility to infection. This effect is observed quantitatively in the reduction of species complexity as measured by the Shannon Index of alpha diversity. Beta diversity analysis indicates that microbial communities associated with GLYPH-treated mosquitoes cluster together and are different than those from control mosquito communities. Additionally, we show that GLYPH'S primary degradation product, AMPA, inhibits melanization. Intriguingly AMPA does not to perturb the microbiome of honeybees (Blot et al., 2019).

In summary, GLYPH's interference with melanization could have considerable environmental impact given that its concentration can vary widely, from over 50 mM at time and at site of application to under 1 nM in runoffs from application sites (Bott et al., 2008; Brauman et al., 2011; Edwards et al., 1980). To illustrate the complexities of the effects of GLYPH on the biosphere, we note that GLYPH also inhibits fungal melanin, a virulence factor in many pathogenic fungi. Melanin protects fungi against predators such as amoeba (Steenbergen et al., 2001; Hillmann et al., 2015). Therefore, inhibition of melanin could make fungal populations more vulnerable to predation, reduce their populations, and alter microbial composition of soils. Consequently, GLYPH may have pleiotropic effects on both microbial virulence and invertebrate immunity through its effects on melanin synthesis. The net result of those dual effects is likely to vary depending on the herbicide concentration and impacts on each particular host-microbe relationship. At some concentrations, GLYPH's inhibition of melanization could make fungi more vulnerable to environmental conditions, which could in turn reduce human infections. At other concentrations, GLYPH could inhibit melanin production in insects, making them more susceptible to pathogens due to reduced immune competence, which could have protean consequences for human health ranging from ecosystem disruption to altered vector competency of human pathogens. Importantly, we provide evidence that GLYPH enhances *A. gambiae* susceptibility to the human malaria parasite. A strong immune response is vital for insect survival. Insects are pivotal members of the world's ecosystems, essential to maintaining proper function and they ensure human food security, yet insect biomass has decreased catastrophically in recent decades (Hallmann et al., 2017), a phenomenon that has been called the "insect apocalypse" (Jarvis, 2018). While there are several factors that likely contribute to this decline, intensive agricultural practices, including the increased use of chemicals such as GLYPH, have been identified as important contributing factors. Understanding the mechanisms by which compounds such as GLYPH might impact insect biomass is important, as they have both direct and indirect impacts on human health. Our work showing that GLYPH inhibits insect

473 melanogenesis highlights another facet by which a compound intended as an herbicide could
474 have pleiotropic ecosystem effects with potential impacts on human health.
475
476 **ACKNOWLEDGEMENTS**
477 We would like to acknowledge Dr. Gene Fridman in the Johns Hopkins School of
478 Medicine for lending the use of the Fridman lab's Metrohm Autolab potentiostat for use in the
479 cyclic voltammetry experiments. We would like to thank the Johns Hopkins Malaria Research
480 Institute and the Department of Molecular Microbiology and Immunology Insectary Core. We
481 would also like to thank the entire Casadevall Lab for their suggestions and inputs during
482 conversations and their feedback during lab meetings and presentations. DFQS, EC, and AC
483 are funded by the Johns Hopkins Malaria Research Institute Pilot Grant Casadevall_123,
484 DFQS, EC, and AC are funded by NIAID R01 AI052733. DFQS has been funded by NIH grants
485 5T32GM008752-18 and 1T32AI138953-01A1.
486
487 **AUTHOR CONTRIBUTIONS**
488 Conceptualization, D.F.Q.S, E.C., R.T., A.J.B., N.A.B., A.C.; Methodology, D.F.Q.S, E.C., R.T.,
489 A.J.B., N.A.B., A.C.; Software A.J.B.; Formal analysis, D.F.Q.S., A.J.B.; Investigation, D.F.Q.S.,
490 E.C., A.J.B., N.A.B.; Resources, R.T., N.A.B., A.C.; Data curation, D.F.Q.S., A.J.B.; Writing –
491 original draft, D.F.Q.S., Writing – reviewing & editing, D.F.Q.S, E.C., R.T., A.J.B., N.A.B., A.C.;
492 Visualization, D.F.Q.S., A.J.B., Supervision, E.C. R.T., N.A.B., A.C.; Project administration,
493 D.F.Q.S., E.C., A.J.B., N.A.B., A.C.; Funding acquisition, E.C., N.A.B., A.C..
494
495 **DECLARATION OF COMPETING INTERESTS**
496 The authors declare no competing interests.
497
498 **STAR METHODS**
499
500 **Lead Contact Statement**
501 Further information and requests for resources and reagents should be directed to and will be
502 fulfilled by the Lead Contact, Arturo Casadevall (acasade1@jh.edu).
503 **Material Availability Statement**
504 This study did not develop any unique reagents.
505 **Data and Code Availability Statement**
506 The 16S rRNA sequencing datasets generated during this study are available at Mendeley Data
507 at DOI:10.17632/6ymh76hmzm.1, and the datasets from the remaining experiments are
508 available at Mendeley Data at DOI:10.17632/xndcmbn6wd.1.

Biological materials

Galleria mellonella larvae were obtained through Vanderhorst Wholesale Inc, St. Marys, Ohio, USA. *Cryptococcus neoformans* strain H99 (serotype A) was kept frozen in 20% glycerol stocks and subcultured into Sabouraud dextrose broth for 48 h at 30°C prior to each experiment. The yeast cells were washed twice with PBS, counted using a hemocytometer (Corning, Inc), and adjusted to 10^6 cells/ml.

Anopheles gambiae (Keele strain) mosquitoes were maintained on sugar solution at 27°C and 70% humidity with a 12 h light to dark cycle according to standard rearing condition. *Plasmodium falciparum* NF54 (Walter Reed National Military Medical Center, Bethesda) infectious gametocyte cultures were provided by the Johns Hopkins Malaria Research Institute Parasite Core Facility and were diluted to 0.05% gametocytemia before feeding to the mosquitoes using an artificial membrane feeder.

Compound and Dilution Preparation

Each compound, including the glyphosate (Millipore Sigma, Product #45521), was prepared in 300 mM stock solution in Milli-Q and brought to a pH of 5.5, and 20 µl of each compound was serially diluted 1:2 in PBS, with a compound-free control. When all reaction components are added, the final concentrations of the drug dilutions were 33.33, 16.67, 8.33, 4.17, 2.08, 1.04, 0.52, and 0 mM.

Dopaquinone Formation MBTH Assay

MBTH reaction mixtures were prepared as previously described (Winder and Harris, 1991). This mixture is warmed at 42°C to help solubilize the components. Then, 5 µl of 2 µg/ml Mushroom Tyrosinase (Sigma, Product #T382) and 20 µl of 20 mM L-DOPA are added to the MBTH solution, and 160 µl of the solution is immediately added to each well containing compounds. The plate was read at an absorbance of 505 nm for 30 min at 30°C, and read again at 1 h and overnight. The DQ levels are determined by the formation of the bright pink adduct between the quinone and the MBTH.

Dopachrome and Melanin Measurements

PO activity was determined as previously described (Cornet et al., 2013), using mushroom tyrosinase instead of PO. The formation rate of dopachrome is measured as the maximum velocity of this reaction, and the dopachrome levels are measured as the absorbance at 490 nm after 30 min as the absorbance values plateau. Melanin levels are measured as the absorbance at 490 nm after the reaction has continued for 5 d in the dark at room temperature.

Free-Radical Scavenging ABTS Assay

ABTS solution was prepared as previously described (Maurya and Devasagayam, 2010). To test the radical-scavenging capability of the compounds, 10 µl of the compounds were serially diluted in a 96 well plate as previously described, and 90 µl of diluted ABTS was added to each well. The 734 nm absorbance was measured immediately, after 10 min, 1 h, and 2 h. In kinetics experiments, absorbance readings were taken every two minutes for 5 h.

To measure the radical scavenging capacity of the synergistic compounds and L-DOPA mixtures, ABTS was prepared and diluted in Milli-Q water. In each well, 5 µl of compound stocks were added with either 5 µl of water or 5 µl of 500 µM L-DOPA. Next, 90 µl of ABTS solution was added to the well, and the absorbance was read immediately at 734 nm. Synergy was calculated from this data using the following formula:

(ΔAbs 734 Compound Alone + ΔAbs 734 L-DOPA Alone) /

(ΔAbs 734 Compound with L-DOPA)

Glyphosate Effect on L-DOPA

To determine if L-DOPA is reacting with GLYPH, we analyzed by NMR. We diluted 300 mM stock of GLYPH in water to 60 mM (10 mg/ml) in D_2O, prepared 20 mM (4 mg/ml) L-DOPA in D_2O, and prepared two mixtures of GLYPH and L-DOPA: one with 20 mM (4 mg/ml) L-DOPA and 60 mM (10 mg/ml) of GLYPH in D_2O, and another with a low concentration of 1 mg/ml for both compounds equaling 5 mM L-DOPA and 6 mM GLYPH. We then performed ^{31}P-NMR and ^{1}H-NMR on these samples.

Glyphosate Effect on Tyrosinase

To determine the tyrosinase kinetics with GLYPH as an inhibitor, we serially diluted 155 µl of 20 mM L-DOPA in Milli-Q water. To each dilution of L-DOPA we added 20 µl of GLYPH diluted in PBS and 5 µl of 2 µg/ml mushroom tyrosinase to the reaction mix. In order to account for non-enzymatic oxidation of L-DOPA, we ran an experiment in parallel, in which we added 5 µl of Milli-Q water instead of tyrosinase. The reaction mix was kept at 30°C for 24 h. The plate was read at 490 nm. To calculate “enzyme-specific” oxidation of L-DOPA, the no enzyme values were subtracted from the tyrosinase rows. The kinetics curve is plotted as a function of absorbance after 24 h of reaction time versus concentration of L-DOPA.

We tested if tyrosinase concentration has an effect on the percent inhibition of the reaction. We prepared dilutions of tyrosinase. We added 5 µl of each dilution to a 96-well plate, and added 135 µl of Milli-Q water, 20 µl of 20 mM L-DOPA, and 20 µl of GLYPH in PBS. We measured maximum velocity of this reaction at 490 nm. The difference in velocities and percent inhibition reported were calculated by difference = $V_{max\ water} - V_{max\ glyph}$, and percent inhibition = $100*(V_{max\ glyph}/V_{max\ water})$.

To determine if GLYPH irreversibly affects tyrosinase activity, 450 µl of 20 µg/ml mushroom tyrosinase was prepared in 450 µl of 50 mM sodium phosphate buffer, pH 7, either with 50 µl of 300 mM GLYPH, or 50 µl of Milli-Q water. The enzyme solution was loaded into a hydrated 10,000 MWCO Slide-a-lyzer dialysis cassette (Thermo Scientific), and the enzyme solutions were dialyzed in a 50 mM sodium phosphate buffer at 4°C, according to the manufacturer's protocol. Protein concentrations were measured and normalized using sodium phosphate buffer. To measure the kinetics of the control enzyme versus the treated enzyme, a kinetics assay was performed as previously described. Each reaction's maximum velocity is determined and plotted.

Copper Rescue of Melanin Inhibition

As previously described, serial dilutions of GLYPH were arrayed in eight rows; one row per copper ion concentrations to be tested. Copper sulfate was prepared and serially diluted and 10 µL of the copper solution is added to each well containing the GLYPH dilution. To each well 150 µL of reaction mix (125 µL of Milli-Q water, 20 µL of 20 mM L-DOPA, and 5 µL of 2 µg/mL mushroom tyrosinase (5 µl of water used for auto-oxidation experiments) was added. The final copper ion concentrations were 400, 200, 100, 50, 25, 12.5, 6.25, and 0 µM. The DC and melanin measurements are reported as previously described.

Cyclic Voltammetry

Cyclic voltammetry was performed using a Metrohm Autolab potentiostat (Switzerland), 3 mm Glassy Carbon working electrode, 10 mm x 10 mm x 0.1 mm platinum plate counter electrode, and an Ag/AgCl reference electrode in 3 M KCl solution. Solutions were prepared in 0.1x PBS (Difco) at a pH 6.00, adjusted with NaOH and HCl. 10 mL of L-DOPA solution was freshly prepared in this buffer, and 1 mL of GLYPH, glycine, water, etc, solution at pH 6.00 were added to the L-DOPA. Readings were done at a scan rate of 50 mV/s at intervals of 5 mV steps. Glassy carbon electrode was washed and polished between readings with slurry of alumina powder and water on cloth pads.

***Galleria mellonella* Hemolymph Extraction and Phenol Oxidase activity**

Healthy (active and cream-colored) larvae were cold anesthetized, punctured in their proleg with 18G needle and pressure was applied to the larvae to promote bleeding of hemolymph. Hemolymph was collected from larvae directly into an eppendorf tube. Anticoagulants were not used as they might interfere with the melanization process.

For automelanization experiments, hemolymph was diluted 1:10 in PBS and mixed with a pipette. Then, 160 µl of 1:10 hemolymph is added to 20 µl of GLYPH serially diluted in PBS. The change in absorbance at 490 nm was read and data analyzed as described above.

For experiments with L-DOPA, hemolymph was diluted 1:5 in PBS and mixed by pipette. Experiments were performed as per the PO activity assay in Cornet, Gandon, and Rivera (2013).

In order to test the effect of GLYPH on hemocytes viability, hemolymph was diluted 1:2 with anticoagulation buffer (Rodrigues et al., 2010), as melanization was not of importance for this experiment. Hemocytes were pelleted and suspended in anticoagulation buffer. GLYPH was added to an aliquot of hemocytes in solution and incubated with mixing on a rocker at 30°C for 15 min. Hemocyte viability was assessed by 0.02% trypan blue staining and enumeration of stained (dead) versus unstained (alive) hemocytes with a hemocytometer.

***Galleria mellonella* Infection and Survival**

Healthy larvae weighing between 175 and 225 mg were selected, and starved overnight. Groups of larvae were injected with 10 µl of PBS or 10 µl of 1 mM sterile GLYPH in PBS. Larvae were monitored and left to recover for 5 h. Larvae were then injected with 10 µl of sterile PBS or injected with 10^4 *Cryptococcus neoformans* yeast cells per larva. Due to the low concentration of GLYPH administered to the larvae, their volume of hemolymph, and their body volume, we believe the approximate concentration of GLYPH is below the concentrations required to inhibit *C. neoformans* growth (Nosanchuk et al., 2001). *G. mellonella* larvae and pupae were kept at 30°C and monitored daily for survival for 14 d. Survival was assessed by movement upon stimulus with a pipette.

***Anopheles gambiae* Phenol oxidase activity**

PO activity assays were performed as previously described (Cornet et al., 2013). Experiments were done in biological triplicate with different batches of mosquitoes, as well as in technical triplicate per biological replicate of 3 batches of 10 mosquitoes.

***Anopheles gambiae* Phenol oxidase activity**

Adult female mosquitoes of *A. gambiae* Keele strain were raised on 10% sucrose for three days post-emergence. On the third day, females were sorted and provided a cotton swab with 10% sucrose mixture with GLYPH. Survival was monitored daily for 14 days.

Anopheles gambiae* infection with *Plasmodium falciparum

Adult female mosquitoes (3-4 days old) of *A. gambiae* Keele strain were sorted and drugged as described above. On the fifth day of GLYPH exposure, mosquitoes were provided a blood meal containing *P. falciparum.* Blood-fed engorged mosquitoes were sorted on ice and fed 10% sucrose *ad libitum* for 8 d. Midguts were dissected and stained with 0.2% Mercurochrome solution and oocysts were enumerated using a 20X objective with light microscopy.

644 ***Anopheles gambiae* Microbiome Analysis**

645 Adult female mosquitoes (3-4 days old) of *A. gambiae* Keele strain were sorted and
646 drugged as described above. On the fifth day of GLYPH exposure, mosquitoes were sterilized in
647 ethanol for 2 minutes, washed, and dissected in sterile PBS. The midguts were removed, placed
648 in 500 µl sterile PBS on ice, homogenized, diluted, and plated on LB agar plates. Plates were
649 incubated at 30°C for three days and individual colonies were counted. Each experiment used
650 10-20 mosquitoes per condition, and the experiment was performed three independent times.
651 For the 16S rRNA sequencing studies, mosquitoes were reared, drugged, and then
652 midguts were dissected as described above, with five individual midguts per condition. DNA was
653 extracted from frozen mosquito samples using the Lucigen EpiCentre MasterPure DNA
654 extraction kit. The bacterial 16S rRNA gene was amplified by PCR, and sample-specific Illumina
655 adapters were ligated to the PCR products. PCR products from multiple samples were pooled
656 and sequenced on the Illumina MiSeq platform. Data were then analyzed using mothur (Schloss
657 et al., 2009) to construct contigs to align forward and reverse reads, remove ambiguous bases
658 and chimeric regions, align sequences to the Silva 16S V4 reference database, and cluster
659 reads into 3% operational taxonomic units (OTUs). Sequences derived from known
660 contaminants were selectively removed. Alpha and beta diversity measurements were
661 performed using the Shannon diversity index and Bray-Curtis dissimilarity distance respectively.
662 Bray-Curtis distances were graphed on principal coordinates analysis (PCoA) plots in two
663 dimensions. Taxa and PCoA graphs were produced using MicrobiomeAnalyst (Chong et al.,
664 2020; Dhariwal et al., 2017).
665
666 **FIG. LEGENDS**
667 **Fig. 1. *GLYPH inhibits in vitro Melanin Production.* (A)** GLYPH inhibits formation of DQ
668 produced by tyrosinase-mediated and spontaneous oxidation of L-DOPA. DQ is indicated by the
669 absorbance of an MBTH-DQ adduct pigment at 505 nm. Absorption levels are shown relative to
670 the no GLYPH control with background (MBTH mixture) subtracted after 1 h at 30ºC **(B)** GLYPH
671 decreases the rate of DC formation and inhibits DC production from tyrosinase oxidation of L-
672 DOPA. Rate of DC formation is the reaction V_{max} at 490 nm relative to the V_{max} without GLYPH.
673 DC production is shown as the absorbance at 490 nm relative to the control after 30 min of
674 reaction. **(C)** Melanin production is inhibited by GLYPH with tyrosinase and auto-oxidation of L-
675 DOPA. Melanin levels are measured as the absorbance at 490 nm after 5 d of reaction. Values
676 are depicted relative to the no GLYPH control. Error bars represent ±SD. Each experiment was
677 performed at least three independent replicates.

Fig. 2. ***Phosphate-Containing Compounds Inhibited Melanization Similarly to GLYPH*** GLYPH, *o*-phosphoserine (PS), phosphonoacetic acid (PAA), pyrophosphate (pyro), and phosphoric acid (PA) inhibit DQ formation **(A)**, rate of DC formation **(B)** and DC levels **(C)**, and melanin formation **(D)**, whereas their respective non-phosphate analogs, glycine (gly), serine (ser), and acetic acid (AA) do not inhibit any step of melanization **(A-D)**. (**E)** Auto-oxidation of L-DOPA is inhibited by GLYPH, PS, PAA, Pyro, and PA in a similar manner. The compounds tested (**F)** were diluted in 300 mM stock solution and titrated to pH between 5 and 6. Absorption and rates are shown relative to the internal no drug control. Grayscale bars represent mean absorbance at 490 nm relative to no compound control. Error bars represent ±SD. Each experiment represents at least three independent replicates.

Fig. 3. ***GLYPH Does Not Directly Inhibit Tyrosinase Activity*** **(A).** Tyrosinase activity is not irreversibly inhibited and GLYPH-treated enzyme has normal activity when GLYPH is dialyzed out of solution. **(B)**. GLYPH appears as a non-competitive inhibitor of tyrosinase in Michaelis-Menten kinetics assays measuring the change in absorbance at 490 nm over 24 h compared to the no tyrosinase background. **(C)** The percent inhibition of DC formation rate with all GLYPH treatment remains constant over varying enzyme concentrations. The assay is performed under constant L-DOPA and GLYPH concentrations. **(D)** Adding Cu^{+2} to L-DOPA-tyrosinase reactions with GLYPH does not rescue melanin inhibition compared to the GLYPH-free control. (See also Fig. S2) Grayscale bars represent mean absorbance at 490 nm relative to no GLYPH and no copper control. Error bars represent ±SD. Each experiment represents at least three independent replicates.

Fig. 4. ***GLYPH Affects the Oxidative Properties of Melanogenesis.*** (**A)** None of the melanin inhibitors exhibit radical quenching properties in an ABTS assay aside from GLYPH, which shows weak antioxidant properties after several hours in the ABTS solution. Absorbance at 734 nm is an indicator of how much ABTS remains in radical form (not quenched). (**B-C)** Citric acid (CA), a non-radical quenching antioxidant (antioxidant synergist) exhibits similar melanin inhibition as GLYPH and phosphoric acid, another known antioxidant synergist. **(D)** GLYPH, phosphoserine, phosphoric acid, and citric acid show synergy with the antioxidant L-DOPA. The addition of these compounds to L-DOPA enhances its radical quenching abilities by approximately 50%. Black dotted line represents the normalized ABTS absorbance treated with water. The other compounds tested here alone do not show much deviation from this line. The blue dotted line indicates the ABTS solution treated with

L-DOPA alone. ABTS treated with L-DOPA and synergetic compounds together are below this line. (**E)** Average cyclic voltagram showing the changes in oxidation and reduction of L-DOPA and DQ when exposed to 16 mM GLYPH but not water. Numbers correspond to shifted peaks or peaks with less current compared to the water control. Peak 1 corresponds to L-DOPA oxidation (**F**); Peak 2 likely corresponds to DQ reduction (**G**). GLYPH shifts Peak 1 and 2 toward a decreased redox potential and diminishes the current of Peak 1 and 2 in a dose-dependent manner (**H**) - notably decreasing Peak 2 current intensity to the point of non-existence **(I)**. Grayscale bars represent absorbance at 490 nm relative to no compound control. Error bars represent ±SD. Each experiment represents at least three independent replicates. See also Fig. S3 and Supplemental Information.

Fig. 5. ***GLYPH Inhibits G. mellonella Melanization and Increases Infection Susceptibility.*** **(A**) GLYPH inhibits the PO activity of 1:10 dilutions of hemolymph without exogenously added L-DOPA. (**B**). *G. mellonella* larvae drugged with GLYPH solution in PBS and infected 5 h post treatment with 10^4 cells of WT *C. neoformans* die rapidly compared to PBS-treated controls. Death events were recorded daily. AMPA, a primary metabolite of GLYPH, inhibits tyrosinase-mediated (**C**) and *G. mellonella* PO-mediated melanization similar to GLYPH. Error bars represent ±SD. Each infection condition represents survival of 95 animals, over the span of four biological replicates, and six total technical replicates. See also, Fig. S5.

Fig. 6. ***GLYPH Effects on A. gambiae Immune System***. (**A**) GLYPH inhibits PO activity in *A. gambiae* homogenate. (**B**) Low doses of GLYPH enhance the survival of adult mosquitoes, while the higher doses diminish their survival as compared to the control. **(C)** GLYPH treatment increases the susceptibility of the *A. gambiae* to *P. falciparum* infection as measured by oocyst count per midgut. Increased GLYPH doses are associated with increased median oocyst burden. (**D**) There is not a significant difference in the *P. falciparum* infection prevalence between GLYPH-treated and untreated mosquitoes, however, there is a trend of increased infection prevalence in 300 μM and 1 mM GLYPH treatment groups. Enzyme activity represents three biological replicates with three technical replicates for each condition. Survival curves represent 120 animals, across three biological replicates. Parasite infection represents four biological replicates and four separate infections, line indicates median, and differences in parasite burden analyzed for significance using two-tailed non-parametric Mann-Whitney test with each group compared to the control group. Infection prevalence was analyzed for significance using Fischer's exact chi-squared test. See also Fig. S6.

Fig. 7. GLYPH Alters the Composition, but Not Density, of the *A. gambiae* Midgut Microbiome. (**A)** GLYPH does not alter microbial density of the culturable mosquito midgut microbiome (grown on LB agar). Each sample consists of 40-50 individual mosquito midguts over three independent replicates. Error bars represent the mean and ±SD. **(B)** GLYPH alters the composition of the mosquito microbiota, leading to depletion of Entereobacteriacae and a bloom of *Asaia spp.* The GLYPH treatments are associated with a decrease in alpha diversity **(C),** and the GLYPH-treated and control-treated microbiota form distinct populations (**D**). Each treatment group represents 5 individual mosquito midguts. For more information see also Fig. S7.

Fig. S1. *Reaction of GLYPH with L-DOPA.* Representative ^{1}H NMR spectra of 60 mM GLYPH solution in D_2O (**Green**), 20 mM L-DOPA solution in D_2O (**Red)**, and 20 mM L-DOPA mixed with 60 mM GLYPH in D_2O (**Blue**). There appears to be no shift in ^{1}H peaks and no appearance of new peaks, which is indicative of no reaction occurring between the compounds. Data representative of three independent replicates.

Fig. S2. *GLYPH appears to "buffer" copper concentration in solution*. High doses (2-16 mM) of GLYPH prevent the enzymatic activity enhancing effects of lower copper concentration (6.25-25 μM), but high doses of GLYPH also prevent the enzyme inhibitory effects of high copper concentration (100-400 μM)**.** Error bars represent ±SD. Data represents at least three independent replicates.

Fig. S3. *Antioxidant Properties of GLYPH.* (A) Change in absorbance of ABTS solution at 734 nm over time for 33.33 mM GLYPH relative to the no GLYPH control. This indicates GLYPH quenches free radicals over an extended period of time. **(B**) Calculated antioxidant radical scavenging synergy between compounds tested and L-DOPA. Values represent the mean of at least three independent replicates. Error bars represent ±SD.

Fig. S4. *GLYPH inhibits melanin production independent of L-DOPA concentration.* (**A)** Inhibitory concentrations of GLYPH are not affected by L-DOPA concentration. This indicates that GLYPH is not reacting proportionately with L-DOPA as measured by absorbance at 490 nm after 5 d of reaction, relative to the no GLYPH control and with background absorbance subtracted. (**B**) The IC_{50} of GLYPH remains constant at approximately 1 mM relative inhibition of melanin production appears dependent on GLYPH concentration alone, and not on L-DOPA to GLYPH ratio. Error bars represent ±SD. Each experiment represents at least three independent

780 replicates. Grayscale bars represent absorbance at 490 nm relative to no GLYPH control. Red
781 line represents the approximate IC_{50}. Crossed out boxes represent values with no data.
782
783 **Fig. S5. *G. mellonella* Supplemental Data. (A)** Protease inhibitor is added to *G. mellonella*
784 hemolymph to prevent the activation of new phenol oxidase, and to control for any impact that
785 GLYPH may have on phenol oxidase activation cascade, cell viability, and gene expression.
786 The general trend remains the same that GLYPH inhibits phenol oxidase activity with and
787 without protease inhibitor, albeit lower with protease inhibitor due to the lower concentration of
788 activated enzyme. **(B)** PO activity was assessed using exogenous L-DOPA for one batch of *G.*
789 *mellonella,* during these experiments, the lower concentration of GLYPH resulted in increased
790 PO activity as compared to the control. This suggests that there may be some cellular regulation
791 of PO induced by GLYPH. It is possible that the doses of GLYPH tested elicit some cellular
792 response that increases PO expression, secretion, and/or activation as a feedback response to
793 the reduced melanin production. These data represent three independent replicates, but this
794 pattern of enzymatic activity as a function of GLYPH concentration was not seen in subsequent
795 batches of larvae. (**C)** Hemocyte viability was not dramatically affected by concentrations of
796 GLYPH ranging from 100 µM to 10 mM, indicating that our data are likely not artifacts of
797 cytotoxic concentrations of GLYPH. **(D)** Larvae treated with GLYPH and subsequently infected
798 with *lac1Δ* mutant *C. neoformans* strain showed a similar pattern of increased susceptibility as
799 the wild type H99, although the differences in susceptibility with the *lac1Δ* infected larvae are
800 not statistically significant. Error bars represent ±SD. Each experiment represents at least three
801 independent replicates. The PBS mock infection condition represents survival of 95 animals,
802 over the span of four biological replicates, and six total technical replicates. The *lac1Δ* mutant
803 infection represents survival of 75 animals over the span of four biological replicates. The PBS
804 mock infection data is the same as the data in Fig. 5b, as all the infections were done
805 concurrently under the same conditions.
806
807 **Fig. S6. Low efficiency *Plasmodium falciparum* infection of *A. gambiae*** Oocyst count per
808 midgut for mosquitoes treated with or without GLYPH and infected with high-passage
809 *Plasmodium falciparum* gametocyte culture, resulting in a low efficiency infection. Data
810 represents one biological replicate. Dotted black line indicates y=0. Black lines for each
811 condition indicate median oocyst count per midgut. We have chosen not to include the data
812 from this replicate in the data shown in Fig. 6, because the results from this one-off replicate
813 appear due to poorly infectious parasite culture. Additionally, it is difficult to make comparisons

using the low infection burden of the control group with a with the treatment groups, as well other replicates with higher oocyst burdens.

Fig. S7. Figure S7: GLYPH affects the *A. gambiae* microbiome in a dose-independent manner (A) At the class level, GLYPH leads to an enrichment of Alphaproteobacteria and a depletion in Gammaproteobacteria**. (B)** Alpha diversity does not follow a distinctive pattern with increasing GLYPH dose. **(C)** GLYPH-treated and control-treated microbiota cluster separately in ordination space, but the clusters are not dose-dependent.

REFERENCES:

de Aguiar, L.M., Figueira, F.H., Gottschalk, M.S., and da Rosa, C.E. (2016). Glyphosate-based herbicide exposure causes antioxidant defense responses in the fruit fly Drosophila melanogaster. Comparative Biochemistry and Physiology Part C: Toxicology & Pharmacology *185–186*, 94–101.

Almeida, F., Wolf, J.M., and Casadevall, A. (2015). Virulence-Associated Enzymes of Cryptococcus neoformans. Eukaryotic Cell *14*, 1173–1185.

Andreotti, G., Koutros, S., Hofmann, J.N., Sandler, D.P., Lubin, J.H., Lynch, C.F., Lerro, C.C., De Roos, A.J., Parks, C.G., Alavanja, M.C., et al. (2018). Glyphosate Use and Cancer Incidence in the Agricultural Health Study. J. Natl. Cancer Inst. *110*, 509–516.

Bahia, A.C., Dong, Y., Blumberg, B.J., Mlambo, G., Tripathi, A., BenMarzouk-Hidalgo, O.J., Chandra, R., and Dimopoulos, G. (2014). Exploring Anopheles gut bacteria for Plasmodium blocking activity. Environ. Microbiol. *16*, 2980–2994.

Bai, L., Wang, L., Vega-Rodríguez, J., Wang, G., and Wang, S. (2019). A Gut Symbiotic Bacterium Serratia marcescens Renders Mosquito Resistance to Plasmodium Infection Through Activation of Mosquito Immune Responses. Front Microbiol *10*, 1580.

Bailey, S.I., and Ritchie, I.M. (1985). A cyclic voltammetric study of the aqueous electrochemistry of some quinones. Electrochimica Acta *30*, 3–12.

Bando, H., Okado, K., Guelbeogo, W.M., Badolo, A., Aonuma, H., Nelson, B., Fukumoto, S., Xuan, X., Sagnon, N., and Kanuka, H. (2013). Intra-specific diversity of Serratia marcescens in Anopheles mosquito midgut defines Plasmodium transmission capacity. Scientific Reports *3*, 1–9.

Barbosa, E.R., Costa, M.D.L. da, Bacheschi, L.A., Scaff, M., and Leite, C.C. (2001). Parkinsonism after glycine-derivate exposure. Movement Disorders *16*, 565–568.

Benbrook, C.M. (2012). Impacts of genetically engineered crops on pesticide use in the U.S. -- the first sixteen years. Environ Sci Eur *24*, 24.

849 Benbrook, C.M. (2016). Trends in glyphosate herbicide use in the United States and
850 globally. Environ Sci Eur *28*.

851 Blot, N., Veillat, L., Rouzé, R., and Delatte, H. (2019). Glyphosate, but not its metabolite
852 AMPA, alters the honeybee gut microbiota. PLOS ONE *14*, e0215466.

853 Borovansky, J., and Riley, P.A. (2011). Melanins and Melanosomes: Biosynthesis, Structure,
854 Physiological and Pathological Functions (John Wiley & Sons).

855 Bott, S., Tesfamariam, T., Candan, H., Cakmak, I., Römheld, V., and Neumann, G. (2008).
856 Glyphosate-induced impairment of plant growth and micronutrient status in glyphosate-
857 resistant soybean (Glycine max L.). Plant Soil *312*, 185.

858 Brauman, K.A., Flörke, M., Mueller, N.D., and Foley, J.A. (2011). Widespread Occurrence of
859 Glyphosate and its Degradation Product (AMPA) in U.S. Soils, Surface Water, Groundwater,
860 and Precipitation, 2001-2009. AGU Fall Meeting Abstracts *44*, H44A-08.

861 Chen, C.C., and Chen, C.S. (1995). Brugia bahangi: Effects of Melanization on the Uptake of
862 Nutrients by Microfilariae in Vitro. Experimental Parasitology *81*, 72–78.

863 Choe, E., and Min, D.B. (2009). Mechanisms of Antioxidants in the Oxidation of Foods.
864 Comprehensive Reviews in Food Science and Food Safety *8*, 345–358.

865 Chong, J., Liu, P., Zhou, G., and Xia, J. (2020). Using MicrobiomeAnalyst for comprehensive
866 statistical, functional, and meta-analysis of microbiome data. Nature Protocols *15*, 799–821.

867 Christensen, B.M., Li, J., Chen, C.-C., and Nappi, A.J. (2005). Melanization immune responses
868 in mosquito vectors. Trends in Parasitology *21*, 192–199.

869 Cirimotich, C.M., Dong, Y., Clayton, A.M., Sandiford, S.L., Souza-Neto, J.A., Mulenga, M., and
870 Dimopoulos, G. (2011). Natural Microbe-Mediated Refractoriness to Plasmodium Infection
871 in Anopheles gambiae. Science *332*, 855–858.

872 Cornet, S., Gandon, S., and Rivero, A. (2013). Patterns of phenoloxidase activity in
873 insecticide resistant and susceptible mosquitoes differ between laboratory-selected and
874 wild-caught individuals. Parasites & Vectors *6*, 315.

875 Dhariwal, A., Chong, J., Habib, S., King, I.L., Agellon, L.B., and Xia, J. (2017).
876 MicrobiomeAnalyst: a web-based tool for comprehensive statistical, visual and meta-
877 analysis of microbiome data. Nucleic Acids Res. *45*, W180–W188.

878 Dill, G.M. (2008). Glyphosate-resistant crops: history, status and future. Pest Management
879 Science *61*, 219–224.

880 Dong, Y., Manfredini, F., and Dimopoulos, G. (2009). Implication of the Mosquito Midgut
881 Microbiota in the Defense against Malaria Parasites. PLoS Pathog *5*.

882 Duke, S.O., and Powles, S.B. (2008). Glyphosate: a once-in-a-century herbicide. Pest
883 Management Science *64*, 319–325.

884 Dzhavakhiya, V., Voinova, T.M., Popletaeva, S., Statsyuk, N., Mikityuk, O., Nazarova, T.A., and
885 Shcherbakova, L. (2016). Some natural and synthetic compounds inhibiting the
886 biosynthesis of aflatoxin B1 and melanin in Aspergillus flavus.
887 SEL'SKOKHOZYAISTVENNAYA BIOLOGIA *51*, 533–542.

888 Edwards, W.M., Triplett, G.B., and Kramer, R.M. (1980). A Watershed Study of Glyphosate
889 Transport in Runoff 1. Journal of Environmental Quality *9*, 661–665.

890 El-Shenawy, N.S. (2009). Oxidative stress responses of rats exposed to Roundup and its
891 active ingredient glyphosate. Environmental Toxicology and Pharmacology *28*, 379–385.

892 Fotouhi, L., Tammari, E., Asadi, S., Heravi, M.M., and Nematollahi, D. (2009). Estimation of
893 heterogeneous rate constants of reaction of electrochemically generated o-benzoquinones
894 with various nucleophiles containing thiol group. International Journal of Chemical Kinetics
895 *41*, 426–431.

896 García-Borrón, J.C., and Sánchez, M.C.O. (2011). Biosynthesis of Melanins. In Melanins and
897 Melanosomes, (John Wiley & Sons, Ltd), pp. 87–116.

898 Gianessi, J.C.& L. (1999). Herbicide Tolerant Soybeans: Why Growers Are Adopting
899 Roundup Ready Varieties.

900 Glass, R.L. (1984). Metal complex formation by glyphosate. J. Agric. Food Chem. *32*, 1249–
901 1253.

902 González-Santoyo, I., and Córdoba-Aguilar, A. (2012). Phenoloxidase: a key component of
903 the insect immune system. Entomologia Experimentalis et Applicata *142*, 1–16.

904 Gordon, M.H. (1990). The Mechanism of Antioxidant Action in Vitro. In Food Antioxidants,
905 B.J.F. Hudson, ed. (Dordrecht: Springer Netherlands), pp. 1–18.

906 Gouagna, L.C., Gouagna, L.C., Mulder, B., Mulder, B., Noubissi, E., Noubissi, E., Tchuinkam, T.,
907 Tchuinkam, T., Boudin, C., Boudin, C., et al. (1998). The early sporogonic cycle of
908 Plasmodium falciparum in laboratory-infected Anopheles gambiae: an estimation of
909 parasite efficacy. Tropical Medicine & International Health *3*, 21–28.

910 Güngördü, A. (2013). Comparative toxicity of methidathion and glyphosate on early life
911 stages of three amphibian species: Pelophylax ridibundus, Pseudepidalea viridis, and
912 Xenopus laevis. Aquatic Toxicology *140–141*, 220–228.

913 Guyton, K.Z., Loomis, D., Grosse, Y., Ghissassi, F.E., Benbrahim-Tallaa, L., Guha, N., Scoccianti,
914 C., Mattock, H., and Straif, K. (2015). Carcinogenicity of tetrachlorvinphos, parathion,
915 malathion, diazinon, and glyphosate. The Lancet Oncology *16*, 490–491.

916 Hallmann, C.A., Sorg, M., Jongejans, E., Siepel, H., Hofland, N., Schwan, H., Stenmans, W.,
917 Müller, A., Sumser, H., Hörren, T., et al. (2017). More than 75 percent decline over 27 years
918 in total flying insect biomass in protected areas. PLoS ONE *12*, e0185809.

919 Hillmann, F., Novohradská, S., Mattern, D.J., Forberger, T., Heinekamp, T., Westermann, M.,
920 Winckler, T., and Brakhage, A.A. (2015). Virulence determinants of the human pathogenic
921 fungus Aspergillus fumigatus protect against soil amoeba predation. Environ. Microbiol. *17*,
922 2858–2869.

923 Jara, J.R., Solano, F., and Lozano, J.A. (1988). Assays for Mammalian Tyrosinase: A
924 Comparative Study. Pigment Cell Research *1*, 332–339.

925 Jarvis, B. (2018). The Insect Apocalypse Is Here. The New York Times.

926 Jayasumana, C., Gunatilake, S., and Senanayake, P. (2014). Glyphosate, Hard Water and
927 Nephrotoxic Metals: Are They the Culprits Behind the Epidemic of Chronic Kidney Disease
928 of Unknown Etiology in Sri Lanka? Int J Environ Res Public Health *11*, 2125–2147.

929 Jiang, N., Sun, N., Xiao, D., Pan, J., Wang, Y., and Zhu, X. (2009). A copper-responsive factor
930 gene CUF1 is required for copper induction of laccase in Cryptococcus neoformans. FEMS
931 Microbiol Lett *296*, 84–90.

932 Johal, G.S., and Huber, D.M. (2009). Glyphosate effects on diseases of plants. European
933 Journal of Agronomy *31*, 144–152.

934 Kissinger, P.T., and Heineman, W.R. (1983). Cyclic voltammetry. J. Chem. Educ. *60*, 702.

935 Liu, X., Zhang, Z., Cheng, G., and Dong, S. (2003). Spectroelectrochemical and Voltammetric
936 Studies of L-DOPA. Electroanalysis *15*, 103–107.

937 Lupi, L., Bedmar, F., Puricelli, M., Marino, D., Aparicio, V.C., Wunderlin, D., and Miglioranza,
938 K.S.B. (2019). Glyphosate runoff and its occurrence in rainwater and subsurface soil in the
939 nearby area of agricultural fields in Argentina. Chemosphere *225*, 906–914.

940 Madsen, H.E.L., Christensen, H.H., Gottlieb-Petersen, C., Andresen, A.F., Smidsrød, O.,
941 Pontchour, C.-O., Phavanantha, P., Pramatus, S., Cyvin, B.N., and Cyvin, S.J. (1978). Stability
942 Constants of Copper(II), Zinc, Manganese(II), Calcium, and Magnesium Complexes of N-
943 (Phosphonomethyl)glycine (Glyphosate). Acta Chem. Scand. *32a*, 79–83.

944 Marmaras, V.J., Charalambidis, N.D., and Zervas, C.G. (1996). Immune response in insects:
945 the role of phenoloxidase in defense reactions in relation to melanization and
946 sclerotization. Arch. Insect Biochem. Physiol. *31*, 119–133.

947 Mason, H.S. (1948). The chemistry of melanin; mechanism of the oxidation of
948 dihydroxyphenylalanine by tyrosinase. J. Biol. Chem. *172*, 83–99.

949 Maurya, D.K., and Devasagayam, T.P.A. (2010). Antioxidant and prooxidant nature of
950 hydroxycinnamic acid derivatives ferulic and caffeic acids. Food Chem. Toxicol. *48*, 3369–
951 3373.

952 Mercurio, P., Flores, F., Mueller, J.F., Carter, S., and Negri, A.P. (2014). Glyphosate
953 persistence in seawater. Marine Pollution Bulletin *85*, 385–390.

954 Motta, E.V.S., Raymann, K., and Moran, N.A. (2018). Glyphosate perturbs the gut microbiota
955 of honey bees. Proc. Natl. Acad. Sci. U.S.A. *115*, 10305–10310.

956 Mylonakis, E., Moreno, R., Khoury, J.B.E., Idnurm, A., Heitman, J., Calderwood, S.B., Ausubel,
957 F.M., and Diener, A. (2005). Galleria mellonella as a Model System To Study Cryptococcus
958 neoformans Pathogenesis. Infection and Immunity *73*, 3842–3850.

959 Nappi, A.J., and Christensen, B.M. (2005). Melanogenesis and associated cytotoxic reactions:
960 Applications to insect innate immunity. Insect Biochemistry and Molecular Biology *35*,
961 443–459.

962 Nosanchuk, J.D., Ovalle, R., and Casadevall, A. (2001). Glyphosate Inhibits Melanization of
963 Cryptococcus neoformans and Prolongs Survival of Mice after Systemic Infection. J Infect
964 Dis *183*, 1093–1099.

965 Nwani, C.D., Nagpure, N.S., Kumar, R., Kushwaha, B., and Lakra, W.S. (2013). DNA damage
966 and oxidative stress modulatory effects of glyphosate-based herbicide in freshwater fish,
967 Channa punctatus. Environmental Toxicology and Pharmacology *36*, 539–547.

968 Ramsden, C.A., and Riley, P.A. (2014). Tyrosinase: The four oxidation states of the active
969 site and their relevance to enzymatic activation, oxidation and inactivation. Bioorganic &
970 Medicinal Chemistry *22*, 2388–2395.

971 Raper, H.S. (1927). The Tyrosinase-tyrosine Reaction. Biochem J *21*, 89–96.

972 Riley, P.A. (1988). Radicals in Melanin Biochemistry a. Annals of the New York Academy of
973 Sciences *551*, 111–119.

974 Rio, R.V.M., Jozwick, A.K.S., Savage, A.F., Sabet, A., Vigneron, A., Wu, Y., Aksoy, S., and Weiss,
975 B.L. (2019). Mutualist-Provisioned Resources Impact Vector Competency. MBio *10*,
976 e00018-19.

977 Robinson, C. (2012). Teratogenic Effects of Glyphosate-Based Herbicides: Divergence of
978 Regulatory Decisions from Scientific Evidence. Journal of Environmental & Analytical
979 Toxicology *01*.

980 Rodrigues, J., Brayner, F.A., Alves, L.C., Dixit, R., and Barillas-Mury, C. (2010). Hemocyte
981 Differentiation Mediates Innate Immune Memory in Anopheles gambiae Mosquitoes.
982 Science *329*, 1353–1355.

983 Romoli, O., and Gendrin, M. (2018). The tripartite interactions between the mosquito, its
984 microbiota and Plasmodium. Parasit Vectors *11*, 200.

985 Samsel, A., and Seneff, S. (2016). Glyphosate pathways to modern diseases V: Amino acid
986 analogue of glycine in diverse proteins. Journal of Biological Physics and Chemistry *16*, 9–
987 46.

988 Saunders, L.E., and Pezeshki, R. (2015). Glyphosate in Runoff Waters and in the Root-Zone:
989 A Review. Toxics *3*, 462–480.

990 Schloss, P.D., Westcott, S.L., Ryabin, T., Hall, J.R., Hartmann, M., Hollister, E.B., Lesniewski,
991 R.A., Oakley, B.B., Parks, D.H., Robinson, C.J., et al. (2009). Introducing mothur: Open-
992 Source, Platform-Independent, Community-Supported Software for Describing and
993 Comparing Microbial Communities. Appl. Environ. Microbiol. *75*, 7537–7541.

994 Seguin, M.-C., and Babizhayev, M.A. (2001). Cosmetic composition useful notably for the
995 skin whitening and melanogenesis inhibiting agent containing such a cosmetic
996 composition.

997 Sinden, R.E., and Billingsley, P.F. (2001). Plasmodium invasion of mosquito cells: hawk or
998 dove? Trends Parasitol. *17*, 209–212.

999 Smith, D.F.Q., and Casadevall, A. (2019). The Role of Melanin in Fungal Pathogenesis for
1000 Animal Hosts. Curr. Top. Microbiol. Immunol. *422*, 1–30.

1001 Smith, R.C., and Barillas-Mury, C. (2016). Plasmodium Oocysts: Overlooked Targets of
1002 Mosquito Immunity. Trends Parasitol. *32*, 979–990.

1003 Smith, R.C., Vega-Rodríguez, J., Jacobs-Lorena, M., Smith, R.C., Vega-Rodríguez, J., and
1004 Jacobs-Lorena, M. (2014). The Plasmodium bottleneck: malaria parasite losses in the
1005 mosquito vector. Memórias Do Instituto Oswaldo Cruz *109*, 644–661.

1006 Steenbergen, J.N., Shuman, H.A., and Casadevall, A. (2001). Cryptococcus neoformans
1007 interactions with amoebae suggest an explanation for its virulence and intracellular
1008 pathogenic strategy in macrophages. Proc. Natl. Acad. Sci. U.S.A. *98*, 15245–15250.

1009 Sviridov, A.V. (2015). Microbial degradation of glyphosate herbicides (Review). Applied
1010 Biochemistry and Microbiology *v. 51*, 188–195.

1011 Tsui, M.T.K., and Chu, L.M. (2003). Aquatic toxicity of glyphosate-based formulations:
1012 comparison between different organisms and the effects of environmental factors.
1013 Chemosphere *52*, 1189–1197.

1014 Urabe, K., Aroca, P., Tsukamoto, K., Mascagna, D., Palumbo, A., Prota, G., and Hearing, V.J.
1015 (1994). The inherent cytotoxicity of melanin precursors: A revision. Biochimica et
1016 Biophysica Acta (BBA) - Molecular Cell Research *1221*, 272–278.

1017 Uren Webster, T.M., and Santos, E.M. (2015). Global transcriptomic profiling demonstrates
1018 induction of oxidative stress and of compensatory cellular stress responses in brown trout
1019 exposed to glyphosate and Roundup. BMC Genomics *16*, 32.

1020 Wang, Y., Aisen, P., and Casadevall, A. (1995). Cryptococcus neoformans melanin and
1021 virulence: mechanism of action. Infect. Immun. *63*, 3131–3136.

1022 Whitten, M.M.A., and Coates, C.J. (2017). Re-evaluation of insect melanogenesis research:
1023 Views from the dark side. Pigment Cell & Melanoma Research *30*, 386–401.

1024 Whitten, M.M.A., Shiao, S.H., and Levashina, E.A. (2006). Mosquito midguts and malaria: cell
1025 biology, compartmentalization and immunology. Parasite Immunology *28*, 121–130.

1026 Winder, A.J., and Harris, H. (1991). New assays for the tyrosine hydroxylase and dopa
1027 oxidase activities of tyrosinase. Eur. J. Biochem. *198*, 317–326.

1028 Yamada, T., Kremer, R., Castro, P., and W. Wood, B. (2009). Glyphosate interactions with
1029 physiology, nutrition, and diseases of plants: Threat to agricultural sustainability?
1030 European Journal of Agronomy *31*, 111–113.

1031 Yu, R.J., and Scott, E.J.V. (1982). Alpha hydroxyacids, alpha ketoacids and their use in
1032 treating skin conditions.

1033 Yu, R.J., and Scott, E.J.V. (2008). N-(phosphonoalkyl)-amino acids, derivatives thereof and
1034 compositions and methods of use.

1035 Zhao, P., Lu, Z., Strand, M.R., and Jiang, H. (2011). Antiviral, anti-parasitic, and cytotoxic
1036 effects of 5,6-dihydroxyindole (DHI), a reactive compound generated by phenoloxidase
1037 during insect immune response. Insect Biochem. Mol. Biol. *41*, 645–652.

1038